



Aerospace Structures Information and Analysis Center

Aeroservoelastic Design with Distributed Smart Actuation System for High Performance Aircraft

Report No. TR-98-04

December 1998

19990326 070

Approved for Public Release; Distribution is Unlimited

DTIC QUALITY INSPECTED 4

Operated for the Flight Dynamics Directorate by CSA Engineering, Inc.

FOREWORD

This report was prepared by the Aerospace Structures Information and Analysis Center (ASIAC), which is operated by CSA Engineering, Inc. under contract number F33615-94-C-3200 for the Air Vehicles Directorate, Wright-Patterson Air Force Base, Ohio. The report presents the work performed under ASIAC Task No. T- 39 The work was sponsored by the Design and Analysis Branch, Structures Division, Air Vehicles Directorate of the Air Force Research Laboratory at WPAFB, Ohio. The technical monitor for the task was Dr. Narendra Khot of the Design and Analysis Branch. The study was performed by Dr. Hayrani Oz, Professor of Aerospace Engineering at Ohio State University, under contract to CSA Engineering Inc.

This technical report covers work accomplished from July 1997 through December 1998.

Table of Contents

	<u>Page</u>
Summary	1
1. Introduction.....	2
2. Aeroelastic System and its Modal Representation.....	3
3. Independent Modal-Space Control (IMSC) of an Aeroelastic System.....	5
3.1 Modal synthesis for control	7
4. Maneuvering Control by Modal Synthesis	9
4.1 Control with compensators	9
4.2 Control without modal compensators	11
5. Modal Synthesis of the Distributed-Parameter-Control	12
6. Control Powers for the Aeroelastic System.....	13
7. Optimal Approximations to the DPCL-IMSC System	15
8. Work-Energy Quantities	19
9. Optimal Modal Performance Output Allocation.....	21
10. Illustration I: Shaping of a Lifting Surface	22
11. Illustration II: Aeroservoelastic Roll Rate-Maneuvering of a High-Speed Air Vehicle.....	22
12. Conclusion	30
13. Acknowledgement	30
14. References.....	31

List of Tables

<u>Table</u>	<u>Page</u>
1 Properties of DPCL-IMSC and its OPAX and GALAX Approximations via Distributed Actuation for the Composite-Plate Lifting Surface.....	32

List of Figures

<u>Figure</u>	<u>Page</u>
I-1 Design-IMAC(--) and DPCL-IMSC(-), Performance Output	33
I-2 DPCL-IMSC Deformed Wing Surface (mm).....	33
II-1 DPCL (CDM and EVM) and GALAX-IMSC (CDM) Performance Output	34
II-2 DPCL-IMSC Generalized Control Loads.....	34
II-3 DPCL and GALAX-IMSC (ripples), EVM Performance Output	35
II-4 GALAX-IMSC Generalized Control Loads	35
II-5 GALAX-IMSC Control Loads	35

Appendixes

<u>Appendix</u>	<u>Page</u>
A DPCL-IMSC and GALAX-IMSC Computer Results for High-Speed Wing.....	36
B DPCL-IMSC and GALAX-IMSC Computer Results for High-Speed Wing via Optimum Modal Performance Output Allocation for Modes 1, 2, 6	52

Aeroservoelastic design with distributed smart actuation system for high performance aircraft

Hayrani Öz¹

2036 Neil Ave., Bolz Hall, 328, Columbus, Ohio 43210
Aerospace Engineering, The Ohio State University

SUMMARY

This report describes the work done by the author to study the feasibility of shaping lifting surfaces via distributed smart actuation systems to achieve high performance flight configurations. In this report, the focus is on first obtaining and identifying optimal distributed-parameter-control equivalent actuation profiles for desired flight maneuvers by a modal synthesis approach. Subsequently, this distributed-parameter equivalent aeroservoelastic solution is to be implemented via a multitude of spatially-discrete actuators distributed throughout the domain of the lifting surface. The selection of the number and distribution of discrete actuators is to be based on optimal approximation solutions which use the optimal distributed-parameter-control equivalent solution as a guiding design. The insight to solutions are sought by considering the aeroservoelastic interactions among aerodynamics, structural flexibility and control actuators from the perspective of work-energy, control power, and control loading requirements.

The Aeroelastic modal formulation is presented in terms of real modal matrices and modal-state variables. Real bi-orthonormality relationships for aeroelastic modes are given with respect to structural matrices. The solution for distributed-parameter-control of an aeroelastic system is developed by modal synthesis from modal-state-space control inputs. In particular, the globally power optimal Independent Modal-Space Control (IMSC) technique is used for maneuver (set-point) control of an aeroelastic system by a modal-performance-output synthesis approach. Control power functionals for an aeroelastic system are defined for any actuation profile and control design. The known solution for the synthesized distributed-parameter closed-loop aeroelastic system is optimally approximated via a gain distribution error minimization technique integrating the transient and power performance characteristics of the system for implementation by distributed, spatially-discrete actuation profiles. For the same purpose, a Galerkin approximation is also given. Work-energy requirements for aerodynamic, structural and control elements are presented; specifically, whenever a rigid-body coordinate exists the work-energy requirements are identified with respect to rigid-body and flexible coordinates, respectively. A modal performance-output allocation optimization problem is also defined, which minimizes a hybrid measure of control power and elastic strain energy of the structure during aeroelastic control.

The modal synthesis approach for aeroservoelastic maneuvering is illustrated by two examples. The first

¹ Professor, e-mail: oz.1@osu.edu web: <http://www-aaa.eng.ohio-state.edu/~aaa/aerospace>
Telephone: 614 292 3843 fax: 614 292 8290

example is for a composite-plate simulating a wing, to twist the wing tip to a prescribed angle of attack by using different distributed actuation profiles. We present both the distributed-parameter-control solution and its optimal approximations via spatially-discrete distributed actuators. The required warped wing shapes can be affected by the approach by synthesizing through different selections of aeroelastic modes for control design resulting in different control power requirements. We illustrate the warped wing shape for the maneuver studied. The second example illustrates the method for a wing design for which the data was provided by the AFRL/VASD at the WPAFB in Dayton, Ohio. A maneuver to achieve a 90 deg/sec roll-rate in a Mach 2 flight condition at altitude was considered and achieved with satisfactory settling-time. The distributed-parameter-control equivalent solution for the maneuver is presented. The control power, control load, and work-energy requirements are calculated for this solution. The preliminary results indicate that such a roll-rate maneuver can be accomplished through feasible levels of control power, work-energy and control loadings. However, due to the nature of the data provided, the illustration provides the generalized-control loads requirements instead of the distributed-parameter-control loading distribution; for the same reason, only the structural modal coordinates' displacements are given for the steady-state flight configuration achieved for the maneuver (therefore the resulting wing shapes were not simulated in this report). For the given wing data, we were also provided a set of 40 discrete actuators imbedded in the wing ribs by which one could attempt to duplicate the performance of the distributed-parameter-control solution. The preliminary results indicate that the given spatially-discrete distributed actuator configuration would require unreasonably high levels of control power, energy and control forces, and further studies would be required to identify alternate actuator configurations and even aerodynamic parameters via an interdisciplinary approach that can accomplish the maneuver within physically realizable control power, control gains, energy and control forces comparable to the feasible levels of the distributed-parameter-control solution.

Key words: Aeroelasticity, aeroservoelasticity, IMSC, modal control, distributed-parameter-control, control power, optimal gain approximation, wing shaping, distributed actuation control, non-self-adjoint system control

1. INTRODUCTION

Aeroelastic systems are represented by operators/matrices that do not have any symmetry and sign-definiteness properties, they represent non-self-adjoint systems. The associated eigenvalue problem is generally complex and their modal descriptions are traditionally dealt with in terms of complex quantities. The biorthonormality relationships, if they are needed, for such problems are given with respect to a state-space dynamic matrix which has an arbitrary structure and is an odd mixture of all system matrices. Yet, there is always a common tendency in the literature to study these systems in a manner akin to the study of self-adjoint structural systems. Often, orthonormal structural modes are used to transform an aeroelastic system with the admission that the invoked structural modal representation loses its orthonormality properties within the aeroelastic system. On the other hand, identification of orthonormal modes is always important from the control perspective, for the truncation of such orthogonal modes still assures that the properties imparted to the retained modal subspace by the control design remain unaltered after model truncation. For non-orthogonal representations, this assurance does not exist. Hence, aeroservoelastic systems are treated in the literature with the acceptance of the curse associated with a non-orthonormal representation albeit in terms of orthonormal modes of the structure alone.

In this report, we remedy this deficiency in the literature, and recast the aeroservoelastic problem anew in a unique form, and introduce an orthonormal modal representation for the aeroelastic system in terms of real conjugate modal quantities. These aeroelastic system modes have the unique property that they satisfy bi-orthonormality relationships simultaneously both with respect to the aeroelastic system matrices and the structural matrices. Thereon, the aeroservoelastic problem can be dealt with in terms of the orthonormal aeroelastic system modes, and specifically the Independent Modal Space Control (IMSC) technique¹ can be applied to design an optimal distributed-parameter-control for the aeroelastic system to accomplish the control objectives by a modal synthesis approach. We refer to this solution as the distributed-parameter-closed-loop IMSC (DPCL-IMSC) solution.

A DPCL-IMSC solution can be implemented by a variety of distributed, spatially-discrete actuation (and sensing) profiles by using an optimal gain distribution approximation or a Galerkin approximation with a perspective on the control power expenditure and transient behavior²⁻⁶. We extend these concepts to an aeroelastic system with a comprehensive, but concise exposition, and illustrate the approach for twisting of a wing tip to a prescribed angle of attack by distributed actuation profiles, and roll-rate maneuvering of a high speed wing-body configuration.

2. AEROELASTIC SYSTEM AND ITS MODAL REPRESENTATION

An aeroelastic system constitutes an integro-differential distributed-parameter-system (DPS). Regardless of whether the DPS description is explicitly available or not, the equations of motion (EOM) of an aeroelastic system with or without unsteady aerodynamic effects can always be written and explicitly developed in the following spatially-discrete configuration-state-space variable form:

$$M \dot{x} + Gx = X \quad (1)$$

In Eq.(1) the n_s -dimensional state variable vector x includes aerodynamic lag state variables if unsteady aerodynamic effects are taken into account, otherwise it consists of only structural state variables. We refer to M as the generalized state-space mass matrix, which is always symmetric and positive-definite. The G matrix is referred to as the generalized aero-elastic-state matrix; it includes all of the structural and aerodynamic mass, damping, gyroscopic (if any), stiffness, and aerodynamic circulatory (Duhamel's integral related) matrices, and therefore is completely arbitrary and sign-indefinite.

Introducing the general solution form $x = v_r e^{\lambda_r t}$ into the homogeneous EOM, we pose the following right (R) and left (L) conjugate aeroelastic eigenvalue problems:

$$[\lambda_r M + G] v_{Rr} = 0 \quad [\lambda_r M^T + G^T] v_{Lr} = 0 \quad (2)$$

The aeroelastic eigenvalue problem, in general, has real and/or complex eigenvalues and real and/or complex eigenvectors as, for example, in the case of maneuvering dynamics of a flexible aircraft. The right and left eigenvectors are bi-orthogonal with respect to the M and G matrices. Once the complex

general conjugate eigenvalue problems are solved, one no longer needs to deal with complex quantities and the problem can be dealt with in terms of real modal matrices and real modal-state variables. To this end, from the eigensolutions, we form the following real aeroelastic conjugate modal matrices and define the conjugate real modal-state variables as:

$$V_R = [|y_{R1} \ z_{R1}| \dots |y_{Rr} \ z_{Rr}| \dots |y_{Rn} \ z_{Rn}|] \quad V_L = [|y_{L1} \ -z_{L1}| \dots |y_{Lr} \ -z_{Lr}| \dots |y_{Ln} \ -z_{Ln}|]$$

$$x(t) = V_R w(t) \quad w = [w_1 \ w_2 \ \dots \ w_r \ \dots \ w_n]^T \quad w_r = [\xi_r(t) \ \eta_r(t)]^T \quad (3)$$

where w is the $n_s = 2n$ vector of modal-states and ξ_r and η_r ($r=1,2,\dots,n$) are a conjugate pair of r -th real modal-states. The notation $|y_r \ z_r|$ denotes a pair of columns formed from the real and imaginary parts, respectively, of the complex eigenvector corresponding to the r -th eigenvalue $\lambda_r = \alpha_r + i \omega_r$. On the other hand, if an eigenvalue λ_r is real, then the notation $|y_r \ z_r|$ for V_R denotes a single column for that eigenvalue formed as the summation $\{ \text{real}(y_r) + \text{imaginary}(z_r) \}$ from the real and imaginary parts of the corresponding eigenvector; and the notation $|y_r \ -z_r|$ for V_L denotes a single column for that eigenvalue formed as the difference $\{ \text{real}(y_r) - \text{imaginary}(z_r) \}$ from the real and imaginary parts of the corresponding eigenvector. Consequently there will be a single real modal-state variable ξ_r or η_r for that eigenvector. Next, we normalize the bi-orthogonal real modal matrices (formed as described) with respect to the state-space mass matrix which yields

$$V_L^T M V_R = 1 \quad -V_L^T G V_R = \text{block-diag} [\Lambda_r]$$

$$[\Lambda_r] = \begin{vmatrix} \alpha_{r1} & \omega_r \\ -\omega_r & \alpha_{r2} \end{vmatrix} \quad \alpha_{r1,2} = \text{Re } \lambda_{r1,2} \quad \omega_r = \text{Im } \lambda_{r1,2} \quad (4)$$

where $r_{1,2}$ denotes the r -th pair of eigenvalues; if complex, they are complex conjugates and real parts are equal $\alpha_r = \alpha_{r1} = \alpha_{r2}$, if the pair is real then α_{r1} and α_{r2} , in general are different and $\omega_r = 0$. If the total number of real eigenvalues is not even (for example, due to truncation), then the single remaining excess eigenvalue after pairing all of the real eigenvalues simply forms a 1X1 diagonal modal-state equation. Note that the modal equations corresponding to all real eigenvalues will indeed be diagonal, but without loss of generality each 2X2 block corresponding to any pair of them can be regarded as a degenerate case for a complex conjugate eigenvalue pair in which the pair has branched into two simple real eigenvalues as in an overdamped oscillator. The general aeroelastic system of Eq.(1) can be transformed via Eqs. (3,4) into a set of uncoupled genuine aeroelastic modal dynamics in terms of a set of conjugate pairs of real modal-states described by:

$$\dot{w}_r = \Lambda_r w_r + f_r^M(t) \quad f_r^M(t) = \begin{bmatrix} f_{yr}^M \\ f_{zr}^M \end{bmatrix} = V_{Lr}^T X = \begin{bmatrix} y_r^T \\ z_r^T \end{bmatrix} X \quad r=1,2,\dots,n \quad (5)$$

where f_r^M are a pair of r-th conjugate modal inputs for the r-th conjugate modal-states. In this modal formulation process, contrary to the common notion, we identified real aeroelastic system modes which are bi-orthonormal with respect to the generalized state-space mass matrix. Bi-orthonormalization can also be accomplished simultaneously with respect to both the structural mass and structural stiffness matrices by also including the structural stiffness matrix alongside the structural mass matrix, in the identity equations in the formation of the M matrix in Eq. (1), in which case M may be termed as the structural matrix (see also Eq. (7) in Sec. 5). To keep $M > 0$, however, one should eliminate any singularity in the structural stiffness matrix. We define the M matrix to consist of structural mass matrix alone, for this results in a better numerical balancing of the M matrix. We also point out that the complex eigenvectors which result from the solutions of the conjugate complex eigenvalue problems as given by Eq.(2) may not necessarily appear as complex conjugates depending on the software package used for solution; but they are indeed complex conjugates pairs.

The aeroelastic modal state-space equations obtained can now be used for aeroelastic control purposes. In particular, we are interested in formulating a distributed-parameter-control solution based on a modal synthesis approach in which each mode is controlled independently of the other modes. This will be followed by the description of two optimal approximation methods for implementing the distributed-parameter-control solution by an arbitrary number of spatially-discrete distributed control actuators integrating the transient behavior and control power considerations.

3. INDEPENDENT MODAL-SPACE CONTROL (IMSC) OF AN AEROELASTIC SYSTEM

In order to keep the focus on the features of the IMSC design approach and not shadow it by the peripheral formulational/computational manipulations, we consider a bare minimum aeroelastic system representation. We assume that the aerodynamic lag dynamics is negligible and the aerodynamic inertia term, if it exists through an aerodynamic mass matrix and structural acceleration vector, is eliminated by substitution of the solution for the acceleration vector as an output equation in terms of the displacement and velocity vectors (the state x) by utilizing the EOM in the structural configuration-space. The ultimate result is that only the generalized structural mass matrix appears and should appear in the inertia term in any formulation with the redefinition of the remaining arbitrary matrices via the necessary algebraic manipulations. Hence, without loss of generality, we consider the following aeroelastic system dynamics in the structural configuration-space.

$$M_S \ddot{q} + C_{SA} \dot{q} + K_{SA} q = Q \quad Q = D F(t) \quad M_S = M_S^T > 0 \quad (6)$$

where q is the n-dimensional generalized coordinates vector which may have both rigid and flexible degrees

of freedom. Typically, Eq.(6), as the starting point, may be the result of a finite-element model of the system in which the flexible coordinates may or may not be the flexible component modal coordinates in vacuo for the flexible domain corresponding to an associated problem. The M_s , C_{SA} , K_{SA} and D represent the generalized structural dynamic mass matrix, aeroelastic damping and/or aeroelastic gyroscopic matrix, aeroelastic stiffness matrix, and D is the transformation matrix from the physical control signal/input variables $F(t)$ to the generalized loads $Q(t)$ in the configuration-space. Whatever its nature, we view Eq.(6) as the evaluation model for the aeroelastic system.

In the sequel, it will be assumed that the D matrix is generated by a number of actuators distributed on and/or embedded in the structural domain. It implicitly inherits all of the information and specifics regarding the associated actuator technology and actuation profile design including orientation of actuation directions, actuator distribution, actuator coverage area or shapes, if any, piezoelectric material properties and polarization profiles. Theoretically speaking, any specified D matrix can be assumed to be realized through tailoring of the actuators utilizing all of the features of the particular actuation technology used. Therefore, we refer to D as the actuation profile matrix. We must also note that the D matrix is relevant for a whole spectrum of control input field distributions, from spatially-discrete point or patched distributions to spatially continuously-distributed (distributed-parameter) input fields. In this study, we do not tailor the actuation profile matrix other than changing the number and locations of the control actuators, since all other issues of a particular actuation technology are theoretically independent of the control design problem beyond the deliverance of a particular- assumed- D matrix.

We write the corresponding state-space equations for Eq.(6) as:

$$\begin{bmatrix} M_s & 0 \\ 0 & M_s \end{bmatrix} \begin{bmatrix} \ddot{q} \\ \dot{q} \end{bmatrix} + \begin{bmatrix} C_{SA} & K_{SA} \\ -M_s & 0 \end{bmatrix} \begin{bmatrix} \dot{q} \\ q \end{bmatrix} = \begin{bmatrix} Q \\ 0 \end{bmatrix}, \quad M \dot{x} + Gx = X, \quad M = M^T > 0 \quad (7)$$

Note the special form of M in terms of the structural mass matrix. In Eq. (7) one can also use the structural stiffness matrix K_s in the bottom half identity equations as discussed in Sec. 2 provided that any singularity in it, is eliminated to keep $M > 0$. Consequently, aeroelastic bi-orthonormality with respect to M will simultaneously satisfy bi-orthonormality with respect to the structural matrices. By following the steps described in Sec.2, we obtain the set of aeroelastic modal dynamics corresponding to Eq.(7):

$$\begin{aligned} \dot{w}(t) &= \Lambda w(t) + f^M(t) & \Lambda &= \text{block-diag}[\Lambda_r] \quad r=1,2,\dots,n \\ f^M(t) &= [f_1^M(t) \dots f_r^M(t) \dots f_n^M(t)]^T & f^M &= V_L^T X \end{aligned} \quad (8)$$

with the associated measurement and controlled performance-output variables described by:

$$y(t) = \sum_{r=1}^n c_r w_r(t) = C w(t) \quad z(t) = \sum_{r=1}^n h_r w_r(t) = H w(t) \quad (9)$$

where C and H are identifiable modal transformation matrices. For simplicity, we assume no disturbances. For a desired system performance, our interest is in designing the modal inputs vector $f^M(t)$ first, as opposed to designing directly a physical input vector in the physical-space (which is an alternative and the traditional approach to the control problem in which the modal inputs are not the designed but derived quantities). The approach we take, therefore, constitutes a genuine modal-space control design. If the modal inputs $f^M(t)$ are designed for desired modal dynamic behavior by any method of one's choice, then one encounters the issue of realizing the designed modal controls by a physical input distribution $f(p,t)$ for implementation purpose, where p denotes the distributed-parameter domain. This necessitates a modal-synthesis procedure for the $f(p,t)$ from the designed modal controls $f^M(t)$.

3.1 Modal synthesis for control

Referring to the Eqs.(4 and 8) the modal-synthesis equation for X appears straightforward:

$$X = [Q^T \ 0^T]^T = M V_R f^M(t) \quad (10)$$

However, for a general arbitrary system, if the modal controls are designed first, Eq (10) imposes a design constraint on the modal control inputs, because whatever the modal inputs are, their synthesis according to Eq.(10) must yield the lower half of the X vector to be zero corresponding to the configuration-state-space identity equations. Hence there must be n synthesis-constraints in the design of the $2n$ modal control inputs $f^M(t)$. The simplest and physically most meaningful way of imposing n such design constraints on the modal vector f^M is to require that for each pair of the modal-state equations only one of the two corresponding modal inputs $f_{y_r}^M$ and $f_{z_r}^M$ be designed arbitrarily and the other one be computed so as to satisfy the synthesis-constraints to assure that the lower half of X is identically zero. In total, then, one must design only n modal control inputs f_z^M or f_y^M . In symmetric structural systems, the synthesis-constraint equations are satisfied identically, and one has freedom to design only one of the modal controls while the other one has to be zero. In gyroscopic systems or arbitrary systems such as an aeroelastic system, the constraints are not satisfied identically and one has to enforce them in the modal-space design approach. Returning to Eq. (10), noting that M is always nonsingular, we observe that the constraint equations are:

$$V_{R1Y} f_Y^M + V_{R1Z} f_Z^M = 0 \quad f_Y^M = -V_{R1Y}^{-1} V_{R1Z} f_Z^M \quad (11)$$

where the subscript 1 denotes the lower partition of the right modal matrix V_R corresponding to the identity equations in the configuration-state-space formulation and f_Y^M and f_Z^M are the n -component vectors of the respective f_{y_r} and f_{z_r} modal inputs. By construct and the nature of the system, the required inverse will always exist. In the first of Eq. (11), one can choose to design f_Y^M or f_Z^M or a mixture of them and write the constraint equation for the remainder ; we choose f_Z^M as the design vector and all f_Y^M are constrained on this choice. In the sequel, one may regard all of the $2n$ - dimensional modal control inputs $f^M(t)$ as the design vector provided that the synthesis-constraints are understood to be implicit in the equations. Hence, the generalized loads Q can be synthesized in the form:

$$\begin{aligned}
Q &= M_S V_{RU} f^M & Q &= M_S V_{RUC} f_z^M \\
V_{RUC} &= -V_{RUY} V_{RIY}^{-1} V_{RIZ} + V_{RUZ}
\end{aligned} \tag{12}$$

where subscripts U,Y,Z refer to the upper partition corresponding to the mass matrix, and the y_r and z_r columns of the matrices, respectively. Using the modal transformation, the modal-state-space equations realized by the synthesized generalized loads Q become:

$$\dot{w}(t) = \Lambda w(t) + B_M f_Z^M(t) \quad B_M = V_{LU}^T M_S V_{RUC} = -[V_{RIY}^{-1} V_{RIZ}]^* \tag{13}$$

where the matrix with an asterisk is obtained by inserting a row of zeros, except for the r-th element which is set to unity corresponding to the r-th input f_{zr}^M , after each row of the matrix product in the brackets. We note that each odd row of B_M is generally full and therefore indicates external coupling of the modes through the modal inputs realized after synthesis.

Associated with Eq. (13), for a particular pair of r-th conjugate modal-states, by disregarding the coupling terms with the other modal inputs, we consider the following form of the uncoupled r-th modal-state equations as the control design model

$$\dot{w}_r = \Lambda_r w_r + B_{Mr} f_{zr}^M(t) \quad r=1,2,\dots,n \tag{14}$$

where B_{Mr} is the 2X1 matrix formed from the pair of elements of the r-th column of B_M corresponding to the r-th modal-state dynamics. One can now perform the modal control design independently for each pair of r-th conjugate modal-states by using their corresponding single modal input f_{zr}^M as feedback function of the r-th modal-states only. This is the approach known as the Independent Modal Space Control (IMSC)¹. Certainly one is now free to use his favorite control theory or tool to design the single modal control input for each uncoupled pair of modal-state dynamics of Eq. (14). The generalized control loads Q can then be synthesized from the designed modal inputs f_{zr}^M for any number of modes according to Eq. (12). It must be kept in mind that although the modal inputs are designed based on Eqs (14), the physically realized modal dynamics with any synthesized inputs is given by Eq.(13). The aforementioned external coupling terms arising through the constraint equations in synthesizing the generalized load Q are in general very weak and therefore have virtually a null effect on the system, and the dynamics of the realized coupled modal system of Eq. (13) becomes practically identical to the dynamics of the system obtained through the set of independent-modal-space control design equations (14), as will be demonstrated by the illustrative examples. Therefore, the modes can be regarded virtually uncoupled for the design process justifying the use of Eq. (14). If the external coupling terms are not weak, the modal synthesis procedure may need to be revisited and alternate synthesis methods be formulated. We do not consider this in this report since the synthesis procedure that is presented above works almost flawlessly.

4. MANEUVERING CONTROL BY MODAL SYNTHESIS

4.1 Control with compensators

One of the features of high performance aeroelastic systems will be their ability to reach desired configurations rapidly by active shaping of aerodynamic surfaces, such as to achieve a high roll-rate by warping of flexible wings. Such target maneuver states can be attained by requiring that a prescribed portion of the desired performance output be achieved by each mode independently of the performances of other modes, which we refer to as the modal- performance-output requirement, such that the synthesis of performances of selected modes yields the desired performance for the system. The performance-output can be written as

$$z(t) = H w(t) = \sum_{r=1}^n z_r(t) \quad z_r(t) = h_r w_r(t) \quad z^*(t) = \sum_{r=1}^n z_r^*(t) \quad (15)$$

where an asterisk denotes a desired single performance-output. To achieve the desired performance-output, we consider an r -th independent modal-space controller with its associated modal-compensator dynamics:

$$\begin{aligned} \dot{w}_r &= \Lambda_r w_r + B_{M_r} f_{z_r}^M && r\text{-th modal-state dynamics} \\ \dot{w}_{cr} &= a_{cr} w_{cr} + b_{cr} e_r && r\text{-th modal compensator} \\ y_{cr} &= c_{cr} w_{cr} + k_{cr} e_r && r\text{-th modal compensator output} \\ f_{z_r}^M &= g_r y_r + g_{cr} y_{cr} && r\text{-th modal control input} \\ y_r &= C_r w_r && r\text{-th modal measurement} \\ z_r &= h_r w_r && r\text{-th modal performance output} \\ e_r &= z_r^* - z_r && r\text{-th modal-performance error} \end{aligned} \quad (16)$$

Each set of these modal dynamics constitute an independent- modal-space-controller in which g_r and g_{cr} are the control gains to be designed by any suitable approach. The prescribed form of the modal compensators is general enough to allow state or output feedback as well as to invoke the internal modeling principle for command and disturbance control. If the chosen modal-compensator dynamics are prescribed as an integrator(s) zero steady-state error can be assured in the closed-loop system, a case of design interest for maneuver control. Note that each modal-compensator is a single input system whereas it may or may not be a first-order dynamics. The modal-space controller dynamics for each mode in the open-loop and closed-loop form can be compacted in the form:

$$\dot{x}_r = A_r x_r + B_r f_{z_r}^M + B_{z_r} z_r^* \quad (17)$$

$$A_r = \begin{bmatrix} \Lambda_r & 0 \\ -b_{cr} h_r & a_{cr} \end{bmatrix} \quad B_r = \begin{bmatrix} B_{Mr} \\ 0 \end{bmatrix} \quad B_{Zr} = \begin{bmatrix} 0 \\ b_{cr} \end{bmatrix}$$

For example, by taking $k_{cr} = 0$ and $c_{cr} = 1$ for a single compensator output and $c_r = 1$ as the 2X2 modal measurement matrix, one can now design $f_{z_r}^M$ as the modal-state feedback input by using eigenvalue-allocation (EVA) or linear quadratic regulator (LQR) design for each modal controller independently. We assume that the modal-states are available for feedback which can be obtained by modal filters¹. With this choice, each modal controller constitutes a third-order dynamics. Furthermore, by choosing $b_{cr} = 1$ and a_{cr} near zero, each modal-compensator behaves as a single integrator resulting in a type-0 control system. Thus, zero steady-state error can be assured for each mode for a step-command input z_r^* , once the stabilizing gains are computed. We illustrate such a design for set-point control in Sec. 8. Note that the command-input z_r^* for each mode can be user specified arbitrarily according to Eq. (15) as long as their sum equals the total desired system performance output z^* . Any set-point control of the system can be accomplished in a variety of combinations of such assigned modal dynamic behaviors. However, command-input z_r^* for each mode for each mode can also be allocated via an optimization procedure as presented in Sec. 10. In this optimum allocation of modal performance outputs, the objective is to minimize a weighted combination of control power and elastic potential energy at the end of the settling-time for the desired maneuver state.

We should note that the modal compensators can also be designed as second order lead-lag minimum or non-minimum phase compensators for each mode depending on the degree and nature of interaction of the modes in the synthesized solution. That is, should the external coupling of the modes prove significant so as to alter the stability characteristics of the independent design modes in the synthesized form, the interactions which are otherwise detrimental on the dynamics of the synthesized system can be affected by higher-order compensators to preserve stability and performance characteristics of the synthesis solution.

It is convenient to represent the system of modal controller equations (16) in an aggregate form

$$\dot{x} = A x + B F(t) + B_z Z^*(t) = (A + B G) x + B_z Z^*(t) = A_{CL} x + B_z Z^*(t) \quad F(t) = G x(t) \quad (18)$$

in which Z^* includes all of the modal command references z_r^* , G denotes a generic control gain matrix and A_{CL} is the closed-loop dynamic matrix for the system. In Eq.(18), $F(t)$ should be viewed as a generic symbol for control signals and may be associated with the modal control signals or the physical control signals, which will be evident from the context of discussion. Note that the form of Eq.(18) holds true for any control design approach. If maneuvering control is a design objective, then Eq.(18) can be transformed into a system of error-state equations in terms of error-states. If the steady-state quantities are denoted by an overbar, the aggregate error-state equations become

$$x_e = A x_e + B F_e(t) = (A + BG) x_e = A_{CL} x_e \quad F_e(t) = G x_e \quad x_{e0} = -\bar{x}$$

$$x_e = x - \bar{x} \quad F_e = F - \bar{F} \quad \bar{x} = -A_{CL}^{-1} B_Z Z^*(t) \quad (19)$$

$$\bar{F} = \bar{G}_Z \cdot Z^*(t) \quad \bar{G}_Z = -G A_{CL}^{-1} B_Z$$

where the subscript 0 denotes the initial error-state assuming that $x_0 = 0$. It is clear now that the controls can be designed for the error-state dynamics alone as a regulation problem, and any stabilizing G will yield the desired performance output with zero steady-state error provided that the modal-compensators assure the required type for the control system such as type-0,1,2 for step, ramp and parabolic commands.

4.2 Control without modal compensators

For the sake of simplicity, control without using compensators is often of interest to study the feasibility of a control task, such as in the case of a desired end-state for the system. The formulation given above can be modified accordingly by deleting the compensator dynamics and states from the above exposition. It must, however, be understood that, without the compensators, zero steady-state errors are not guaranteed in the presence of parameter errors in the system.

In the case of control design without compensators, we denote the modal control input variables $f_{z_r}^M$ on the modal state-space model of the vehicle by an overbar, and carry out the control design according to the following:

$$\dot{w}_r = \Lambda_r w_r + B_{M_r} \bar{f}_{z_r}^M$$

$$\bar{f}_{z_r}^M = f_{z_r}^M + k_a z_r^* \quad f_{z_r}^M = g_r w_r \quad (20)$$

$$\dot{w}_r = \Lambda_r w_r + B_{M_r} f_{z_r}^M + B_{Z_r} z_r^* \quad B_{Z_r} = B_{M_r} k_a$$

$$k_a = z^*/(H A_{CL}^{-1} B_Z Z^*) \quad A_{CL} = \Lambda + B_M G_{MZ}$$

in which $f_{z_r}^M$ is now the portion of the modal input that we design as state-feedback; hence, g_r is the modal control design gain, and the scalar k_a is an amplifier gain on all of the modal command reference inputs z_r^* , which is determined (adjusted) after the modal design control gains are obtained, to render the steady-state total performance output z equal to the desired value z^* . The third equation in Eq.(20) is the counterpart of Eqs.(16), without modal compensator dynamics and G_{MZ} , A_{CL} and B_M are the total modal design gain matrix, closed-loop dynamic matrix and input influence matrix etc. for the aggregate

modal system. For a desired z^* , z_r^* are assigned according to Eq. (15) either manually or according to an optimization problem as discussed in Sec. (10). Note that once the k_a is computed according to the last equation in Eqs. (20), the modal performance outputs z_r^* are essentially scaled by it, such that in the sequel, if the controls are designed without modal compensators, the required modal performance outputs must be understood to be $z_r^{*(NEW)} = k_a z_r^*$. Hence, the following discussions now apply to the system both with or without the modal compensators.

With the modal control inputs designed via the IMSC approach as described, the generalized control load Q can be synthesized as per Eq.(12) and the modal dynamics realized after modal synthesis can be simulated via Eq. (13). However, for a DPS, it still remains to synthesize the physical distributed-parameter- control input field $f(p,t)$ from the modal-controls, which is ultimately the control input to be implemented on the aeroelastic system.

5. MODAL SYNTHESIS OF THE DISTRIBUTED-PARAMETER-CONTROL

The aeroelastic system that is represented by Eq. (1) or (7) has a distributed-parameter displacement field $u(p,t)$ which can be expanded in terms of assumed admissible shape functions $N_r(p)$ ($r=1,\dots,n$) in the form

$$u(p,t) = \sum_{r=1}^n N_r(p) q_r(t) = N(p) q(t) \quad M_s = \int_{D(p)} m(p) N^T(p) N(p) dD(p) \quad (21)$$

where M_s is the n-dimensional structural mass matrix as appears in Eq.(7) and $D(p)$ is the distributed domain of the problem. The controls that are to be physically implemented on the aeroelastic system can also be represented as a distributed-parameter-control input field $f(p,t)$ which yields the n-component generalized control load Q as

$$Q = \int_{D(p)} N(p)^T f(p,t) dD \quad Q = M_s V_{RU} f^M \quad (22)$$

in which the second expression for Q is given by Eq.(12) as synthesized from the designed modal control inputs. Comparing these two expressions and noting the definition of the generalized structural mass matrix, it follows that the distributed-parameter-control field can be synthesized from the modal controls in the form:

$$f(p,t) = m(p) N(p) V_{RU} f^M(t) = m(p) N(p) V_{RUC} f_Z^M(t) \quad (23)$$

which constitutes a spatially continuously distributed control input field since the shape functions are spatially continuous. The synthesized $f(p,t)$ is of the form

$$f(p,t) = \sum_{s=1}^{2n} m(p) \phi_s(p) f_s^M(t) \quad \phi_s(p) = N(p) V_{RUs} \quad (24)$$

in which ϕ_s is the effective s-th aeroelastic eigenfunction and V_{RUs} is the s-th column of the right modal matrix. Referring to Eq.(22), for the modal synthesized distributed-parameter-control field the corresponding actuation profile matrix D and the physical control actuation signals F (t) are identified as

$$D = M_S V_{RUC} \quad F(t) = f_Z^M(t) \quad Q = D F \quad (25)$$

which compares with Eq. (12) and the modal controls are identified as the physical actuation signals. Next, we consider the control powers expended on the aeroelastic system by any control design as per the definitions given in Refs.(2,3)

6. CONTROL POWERS FOR THE AEROELASTIC SYSTEM

The real (control) power expended by any distributed-parameter (control) input field is defined as

$$S_R = \int_t \int_{D(p)} m(p)^{-1} f^2(p,t) dD(p) dt = \int_t Q^T M_S^{-1} Q(t) dt = \int_t F^T(t) D^T M_S^{-1} D F(t) dt \quad (26)$$

These expressions are identical to the ones given in Refs. (2,3) and valid regardless of how the (control) input field is generated/designed. Next, we define the modal (control) power expended on the aeroelastic system by any distributed-parameter-control input field by introducing into Eq.(26) the expansion, Eqs.(24), for the f (p,t) in terms of the modal inputs.

$$S_M = \int_t f^{MT} V_{RU}^T M_S V_{RU} f^M dt \quad (27)$$

this expression is valid for any control design and the f^M would be the modal controls generated by the particular control method. By using the biorthonormality relations, it is easy to see that if the modal controls f^M include all of the modes of the distributed-parameter system or its surrogate evaluation model as in Eqs.(1,7) then $S_R = S_M$. If S_M is computed by using only a subset of the modal inputs such as those of a reduced-order control design model, then $S_R \geq S_{MC}$ where the subscript C denotes the modal power for the reduced-order control design model (CDM). The difference between S_R and S_{MC} corresponds to control power spillover into the uncontrolled modes, hence the control power efficiency for a reduced-order control design model is easily calculated as the ratio of the modal control power to the real control power. In terms of the physical control input signals F (t), the modal control power functional S_{MC} for a reduced-order control design model takes the form

$$S_{MC} = \int_{t_0}^{t_f} Q(t)^T V_{LU}^C V_{RU}^{CT} M_S V_{RU}^C V_{LU}^{CT} Q(t) dt = \int_{t_0}^{t_f} F^T(t) D^T V_{LU}^C V_{RU}^{CT} M_S V_{RU}^C V_{LU}^{CT} D F(t) dt \quad (28)$$

in which the superscript C denotes the set of controlled modes and the subscript U denotes the upper partitions of the modal matrices corresponding to the generalized loads Q. The control powers for the maneuver problem are obtained in the form

$$S_R = S_{RD} + S_{RD*} + S_{RS*} = x_{e0}^T P_R x_{e0} + 2 \int_0^{t_s} \bar{F}^T R_R F_e dt + \int_0^{t_f} \bar{F}^T R_R \bar{F} dt$$

$$S_{MC} = S_{MD} + S_{MD*} + S_{MS*} = x_{e0}^T P_M x_{e0} + 2 \int_0^{t_s} \bar{F}^T R_M F_e dt + \int_0^{t_f} \bar{F}^T R_M \bar{F} dt \quad (29)$$

$$A_{CL}^T P_R + P_R A_{CL} + Q_R = 0 \quad A_{CL}^T P_M + P_M A_{CL} + Q_M = 0$$

$$R_M = D^T V_{LU}^C V_{RU}^{CT} M_S V_{RU}^C V_{LU}^{CT} D \quad Q_M = G^T R_M G$$

$$R_R = D^T M_S^{-1} D \quad Q_R = G^T R_R G$$

S_{RD} and S_{MD} correspond to transient dynamics powers computable through the solution of Lyapunov power equations as given; S_{RD*} and S_{MD*} represent transient command powers due to coupling between steady-state and error-state controls and will vanish after the zero steady-state error is attained. S_{RS*} and S_{MS*} are the steady-state command powers required to achieve and sustain the maneuver. The command powers are ultimately functions of the reference command $z^*(t)$ and can be computed once it is specified. P_R and P_M denote the transient real and modal Lyapunov power matrices due to error dynamics in the reaching phase to the maneuver set-point. t_s denotes the zero steady-state error settling-time for the maneuver, t_f is the maneuver termination time. The subscripts D and S on the control powers denote the transient dynamics control power and steady-state command control power requirements, respectively, for achieving the maneuver. For future reference, it will be convenient to write the modal power functional explicitly in terms of the effective modal control gain matrix in the form

$$S_M = S_{MD} + S_{MD*} + S_{MS*} = \int_{t_0}^{t_f} f^{MT} \bar{R}_M f^{MT} dt = x_{e0}^T P_M x_{e0} + 2 \int_0^{t_s} \bar{f}^{MT} \bar{R}_M f_e^M dt + \int_0^{t_f} \bar{f}^{MT} \bar{R}_M \bar{f}^M dt \quad (30)$$

$$A_{CL}^T P_M + P_M A_{CL} + G_M^T \bar{R}_M G_M = 0 \quad A_{CL} = A + G_M \quad \bar{R}_M = V_{RU}^{CT} M_S V_{RU}^C$$

$$f^M = G_M x \quad f_e^M = G_M x_e \quad \bar{f}^M = -G_M A_{CL}^{-1} B_Z Z^*(t)$$

In concluding, we should note that the control power functionals presented are uniquely defined, dimensionally consistent, genuine control powers; they are not the kind of "control powers" loosely identified in the control literature with a typical quadratic control cost term in an LQR design setting with arbitrarily chosen weighting matrices. The control powers defined herein are not used to design the control inputs; but are used to evaluate the power performance of controls designed by any method whatsoever².³ We also note that the modal control powers introduced in this paper for aeroelastic (or arbitrary systems) differ from the ones introduced in Refs (2,3) where self-adjoint systems were considered. Certainly, the definition given in Refs. (2,3) is a special case of the form given here when the conjugate eigenvalue problems are identical.

The definitions given here for control powers apply for any control approach with any kind of control actuation profile distribution, and therefore are not specific to the IMSC approach discussed in the previous section. However, for any desired control performance, the control powers corresponding to the distributed-parameter-control input profile synthesized via the IMSC approach as discussed in Sec. 5 are the globally minimum control powers among all dynamically similar designs, that is, all designs having the same closed-loop eigenvalue spectrum. We refer to the DPS, in its explicit or implicit form, which is controlled by the distributed-parameter-control input field synthesized from the IMSC designs according to Eq. (22) as the distributed-parameter-closed-loop-IMSC (DPCL-IMSC) system.

In addition to its computational advantages, the globally power optimal feature of a DPCL-IMSC solution makes it an ideal control approach for distributed-parameter-smart structure applications where spatially continuously distributed actuation and sensing can be affected with modal actuators and modal sensors^{1,4}.⁵ However, for practical applications, it is often more desirable to implement the control design by using a multitude of spatially-discrete locally distributed actuators (and sensors). Hence, we now seek to implement and duplicate the dynamic, controlled-output and power performance of the DPCL-IMSC solution for the aeroelastic system by employing a finite but large number of distributed, locally actuated control actuators. To this end, we use the approach presented in Ref. (6) and design optimal approximations to a DPCL-IMSC solution, which is obtained a priori as the ideal design for the control task. For brevity, we refer the reader to Ref. (6) on the development of the approach and include only the design equations as they apply to an aeroelastic system with a more concise perspective and notation.

7. OPTIMAL APPROXIMATIONS TO THE DPCL-IMSC SYSTEM

We assume that a DPCL-IMSC solution has already been obtained for the DPS with its design modal control gains prior to synthesis given in the form

$$f^{M*}(t) = B_M^* f_Z^M(t) = G^* x^* \quad G^* = B_M^* G_{MZ}^* \quad f_Z^M = G_{MZ}^* x^* \quad B_M^* = \text{block-diag} [B_{M_r}] \quad (31)$$

where an asterisk on the matrices indicates the IMSC design quantities, hence G^* is the effective IMSC modal gain matrix and G_{MZ}^* is the designed modal gain matrix for the modal controls f_Z^M . It should be noted that the coupling terms with all other modes are ignored in the B_M^* matrix as defined since their net

effect is expected to be insignificant or null. Hence with this caveat, we compute the transient Lyapunov modal power matrix of this system by Eq. (30) .

$$A_{CL}^{*T} P^* + P^* A_{CL}^* + Q^* = 0 \quad A_{CL}^* = [A + G^*] \quad Q^* = G^{*T} \bar{R}_M G^* \quad (32)$$

where P^* is the transient dynamics modal power matrix . We refer to the system represented by Eqs. (31 , 32) as the design-IMSC. The synthesized distributed-parameter-control field which is also the physically realized control corresponding to this design is given by Eq.(23) and has virtually the same dynamic and power performance as the design-IMSC. Instead of implementing the synthesized distributed-parameter-control in the form given by Eq.(23), we opt to synthesize the controls approximately by using a spatially-discrete distribution of local control actuators while requiring that the transients and the control powers of the approximation be as near those of the distributed-parameter-control IMSC design as possible. Hence, we consider an approximation physical control distribution in the form of localized control shape functions or control loading influence functions multiplied by physical control coordinates or signals $F(t)$:

$$f_a(p,t) = \sum_{k=1}^{ni} m(p) \Psi_k^E(p) F_k(t) = \sum_{k=1}^{ni} \Psi_k(p) F_k(t) = \Psi(p) F(t) \quad (33)$$

where Ψ_k^E is the local control support /shape function and Ψ_k is the local control loading influence function for the k-th actuator and ni denotes the number of actuators, $F_k(t)$ is the physical control signal strength for the k-th actuator. In anticipation of electroelastic actuation, we used superscript E on the control shape functions which are to be realized by the particular actuation technology chosen. We do not consider the details of realization of the control shape or control loading influence functions in this paper and refer the reader to Ref. (1) for specific derivations. Here, we assume the forms of these functions for illustration purposes and that they can be realized for implementation. Furthermore, to preserve generality, it is assumed that the respective control loading influence functions are identified as dimensionless quantities thus rendering the control coordinates/signals $F_k(t)$ to be dimensionally the same as the distributed-parameter input field $f(p,t)$ relevant to the problem. Thus, for the aeroservoelastic control of a lifting surface $F_k(t)$ will conveniently have the units of (control) pressure. Further, in case of piezoelectric actuation as an example of the particular actuation technology used, dividing F_k by a corresponding characteristic polarization (charge/area) or a characteristic charge density (charge/volume) will convert/ scale a control signal strength into electric field strength or voltage potential difference to be applied to the particular actuator. We are to design the signals $F_k(t)$ (which may be precisely referred to as the control coordinates or control degrees of freedom) to approximate the DPCL-IMSC solution by $f_a(p,t)$.

For approximating the DPCL-IMSC solution for control implementation, we consider the control coordinates in the form

$$F = G x \quad F = [F_1 \ F_2 \ \dots \ F_{ni}]^T \quad F_k(t) = \sum_{s=1}^{2n} g_{ks} x_s \quad k=1,2,\dots,ni \quad (34)$$

where G is the $ni \times 2n$ dimensional physical control gain matrix of unknown gain parameters g_{ks} . Note that,

if a reduced-order control design is considered, one only needs to sum over the set of controlled modes.

The synthesized globally optimal distributed-parameter-control IMSC solution and its approximation as represented in the form of Eq. (33) can be written in the form

$$\begin{aligned} f^*(p,t) &= m(p) \varphi(p) G_{SYN} x^*(t) = g^{*T}(p) x^*(t) & G_{SYN} &= B_M G_{MZ} \\ f_a(p,t) &= \Psi(p) G x(t) = g_a^T(p) x(t) \end{aligned} \quad (35)$$

where $g^{*T}(p)$ and $g_a^T(p)$ denote the row vectors of globally optimal distributed-parameter-control gain distribution functions and the locally distributed control gain functions of the approximation, respectively. While the functions $g^*(p)$ are known, the functions $g_a(p)$ are unknown by virtue of the unknown gain parameters g_{ks} . Following the developments presented in Ref. (6), we define the total quadratic control gain distribution error functional for the domain of the problem as:

$$\begin{aligned} S_{ge} &= \int_{D(p)} [g^*(p) - g_a(p, g_{ks})]^T [g^*(p) - g_a(p, g_{ks})] dD(p) \\ &= \int_{D(p)} g_E^T(p, G_{MZ}^*, g_{ks}) g_E(p, G_{MZ}^*, g_{ks}) dD(p) \end{aligned} \quad (36)$$

in which g_{ks} are the design parameters and $g_E(p)$ is the control gain error distribution functions vector. However, one usually has a spatially-discrete description of the DPS such as a finite-element-model, rather than an explicit distributed-parameter-system formulation, that is, the EOM of the form of Eq. (7) are generally the starting point in the configuration-space in terms of generalized coordinates. Hence, alternately and more practically, we can define a generalized quadratic control gain error norm by considering the projection of the control gain error distribution vector onto the configuration-space.

$$S_{EG}^Q = \|E_G^Q\|_F \quad E_G^Q = \int_{D(p)} N^T(p) g_E^T(p, G_{MZ}^*, g_{ks}) dD(p) \quad (37)$$

in which S_{EG}^Q and E_G^Q are the configuration-space gain error norm and the configuration-space gain distribution error matrix, respectively, and F denotes matrix Frobenius norm (F-norm). It can be shown that S_{EG}^Q can be computed in the form:

$$S_{EG}^Q = \|E_G^Q\|_F = E_{GF}^Q = \|M_S V_{RUC} G_{MZ} - D G\|_F \quad D = \int_{D(p)} N^T \Psi(p) dD(p) \quad (38)$$

We now pose the following **optimal approximation (OPAX) problem**:

$$\begin{aligned}
& \text{minimize} && S_{ge} \vee S_{EG}^Q \\
& \text{constraint} && q / (2 p^*) - e \geq 0 \\
& && q = \| Q_M^* + \gamma + \gamma_p P^* \|_F \quad e = \| \sigma(E) \|_F = \| E + \sigma \|_F \\
& && p^* = \| P^* \|_F \quad E = A_{CL} - A_{CL}^* \quad E = E_G + E_p = B G - G^* + E_p
\end{aligned} \tag{39}$$

This is a convex optimization problem with a single inequality constraint describing a stability requirement for the closed-loop approximation system. E is the total error matrix in the modal-state-space between the closed-loop dynamic matrices of the approximation system and the design-IMSC. E is due to a modal-space control gain error matrix E_G and may include a parameter error matrix E_p . Hence, parameter uncertainties can also be dealt with by the optimization problem posed here. We also point out that although the approximation gain matrix G appears as the state gain matrix, output feedback approximations can also be accommodated by this approach since G , in this case, can be regarded as the product of unknown output feedback gains with the measurement/output matrix. The development of the optimization problem is given in Ref. (6). The apriori designed globally optimal-IMSC solution drives the optimal approximation problem. All this simply means that whether distributed actuation and/or presence of parameter uncertainties, the approximation system is to mimic the behavior of an ideal design, the DPCL-IMSC solution. In expressions (39) the matrices γ γ_p σ are positive semi-definite diagonal weighting matrices chosen to tailor the response and the control power performance of the approximate system about the globally optimal IMSC design. In general larger values for σ improve stability; but the larger values of γ and γ_p improve the power performance while degrading stability. Hence, these optimization weighting parameters provide a trade-off between stability and control power performance of the optimum approximation with respect to the DPCL-IMSC design. The optimal approximation approach is applicable for any number of actuators regardless of the order of the control design model.

Galerkin approximation (GALAX): A second approximation technique that has been traditionally used to implement an IMSC design is based on eliminating completely the modal-space gain error E_G between the approximation solution and the DPCL-IMSC solution. Consequently, the design solution and the approximation have exactly the same eigenvalue spectrum. This procedure truly constitutes a Galerkin approximation (GALAX) in which gain error projections onto the subspace of controlled-modal-states are forced to vanish. The approximation gain solution is readily available by setting the modal gain error $E_{G_{SYN}}$ for the synthesized solution equal to zero and solving for G :

$$E_{G_{SYN}} = B G - G_{SYN}^* = 0 \quad G = B^{-1} G_{SYN}^* \quad G_{SYN}^* = B_M G_{MZ}^* \tag{40}$$

in which B_M is given by Eq.(13) for the synthesized-IMSC solution. The Galerkin approximation requires that for exact solution the number of localized actuation signals should be greater than or equal to the dimension of the synthesized modal gain matrix G_{SYN}^* , that is the size of the controlled modal subspace.

The required matrix inversion can be performed via the singular value decomposition of B and constitutes a minimum norm solution for the columns of G . The Galerkin approximation solution has been the popularly known method of implementing an IMSC solution. Although this approach did put a severe restriction on the number of actuators by the measures of the state of the art a decade or so ago, it no longer poses a severe restriction for many electroelastic applications where large number of actuators can be made available exceeding the size of the controlled subspace. Indeed, under such circumstances, given the uncoupled nature and the computational advantages of the IMSC approach, the use of coupled-control¹ techniques and their inherent computational intricacies for control design should induce some reservation.

8. WORK-ENERGY QUANTITIES

Active shaping of a flexible lifting surface for a maneuver performance brings the interplay among the inertial loads, elastic loads, control loads and the aerodynamic loads. It is therefore necessary that one consider the work-energy terms that result from each one of these loads during the maneuver. For example, the question arises whether all of the energy needed for a maneuver should be provided through the control actuators or might it be possible to extract some or all of the energy from the air stream by proper flexing of the lifting surface, thus preserving control power. Hence, it is expedient to evaluate the respective work-energy terms to better understand these aeroservoelastic interactions. We shall assume that for a maneuvering flight, the generalized coordinates (configuration) vector consists of a single rigid-body rotational coordinate (the first generalized coordinate) and the rest of the coordinates are generalized flexible coordinates. The flexible coordinates can be structural modal coordinates, but will not be modal coordinates of the hybrid flight system. Thus, we consider the work-energy terms in terms of generalized coordinates separately as the kinetic energy (due to inertia loads), elastic energy (due to internal elastic loads- elastic potential energy), work done by the control actuators, work done by the external aerodynamic loads proportional to generalized velocities (loosely referred to as the aerodynamic damping work), and the external work done by the aerodynamic loads proportional to generalized displacements (referred to as the aerodynamic stiffness work).

The work-energy equation is obtained by taking the scalar product of the vector form of the EOM, Eq. (6) with the incremental generalized coordinate displacement vector $dq(t)$ and integrating between any arbitrary time interval during the maneuver. Thus denoting by W_{KIN} , W_{FLX} , W_{ARD} , W_{ARS} , W_{ACT} the resulting work terms due to inertia loads, elastic loads, aerodynamic damping and aerodynamic stiffness loads, and actuator loads, respectively, we have:

$$\begin{aligned}
W_{KIN} &= \int_{t_0}^{t_f} F_I^T \dot{q} dt & F_I &= M\ddot{q} & W_{FLX} &= \int_{t_0}^{t_f} F_{FLX}^T \dot{q} dt & F_{FLX} &= K_S q \\
W_{ARD} &= \int_{t_0}^{t_f} F_{ARD}^T \dot{q} dt & F_{ARD} &= C_A \dot{q} & W_{ARS} &= \int_{t_0}^{t_f} F_{ARS}^T \dot{q} dt & F_{ARS} &= K_A q \\
W_{ACT} &= \int_{t_0}^{t_f} Q^T \dot{q} dt & & & W_{KIN} + W_{FLX} + W_{ARD} + W_{ARS} &= W_{ACT}
\end{aligned} \tag{41}$$

The kinetic work (kinetic energy) and the elastic work (strain energy) terms are conservative so that they can be represented in terms of initial and final states only. The aerodynamic and actuator work terms are non-conservative, so they have to be calculated via formal integration. Furthermore, note that just like the external actuator work, the aerodynamic work terms are also external to the flight vehicle, so they more appropriately belong to the RHS in the work - energy equation. According to the way the work terms are defined above, however, a positive actuator mechanical work term implies that actuators do work on the system (this work is thermodynamically negative from the system's perspective; energy is added to the vehicle); whereas positive aerodynamic work terms will imply that the system does work on its surrounding (this is also positive work from the system's perspective; energy is lost to the airstream), conversely a negative aerodynamic work term implies that work is done by the aerodynamic forces on the vehicle. Hence, we write the work-energy equation in the form:

$$\begin{aligned}
T + U_{STR} + W_{ARD} + W_{ARS} &= W_{ACT} \\
T = W_{KIN} &= 1/2 \dot{q}^T(t_f) M_S \dot{q}(t_f) - 1/2 \dot{q}^T(t_0) M_S \dot{q}(t_0) \\
W_{FLX} = U_{STR} &= 1/2 q^T(t_f) K_S q(t_f) - 1/2 q^T(t_0) K_S q(t_0)
\end{aligned} \tag{42}$$

in which the initial states would typically be null, such as at the initiation of the maneuver. Because the energy-work equation pertains to the actual physical system, the energy balance will always be assured if quantities are computed for the evaluation model (EVM) of the controlled system in terms of the configuration-space generalized coordinates serving as the surrogate physical system. On the other hand, if the work terms above are computed based on the reduced-order control design model (CDM) response of the system such as represented by the truncation of aeroelastic modes, they will not necessarily balance according to the above equation due to model truncation.

Another view of the energy-work quantities for the aeroservoelastic system is relevant from the perspective of dynamics and actuator configuration. We consider contributions to the (generalized) work terms, if it

exists, due to the generalized rigid-body rotational coordinate displacement (denoted as the 1st generalized coordinate) and the generalized flexible coordinates displacements. When the system reaches a static equilibrium configuration such as in a steady-state maneuvering rate configuration, the total work done through the rigid-body coordinate displacement by all of its compatible generalized loads in the static configuration must vanish. Accordingly, the total work done through the flexible coordinates displacements by all of their generalized loads in the static equilibrium configuration must also vanish. In reporting the computer simulation results, we refer to the respective calculations as rigid-body-work and flexible-work terms.

It should be noted that when a static maneuvering state is achieved in t_s seconds (maneuver settling-time), the vehicle will have deformed into a new non-trivial static flexible configuration, and the kinetic energy will be due to its steady-state rigid-body rotational rate only, with no contribution from the flexible dynamics due to vanishing of generalized flexible coordinates velocities in the deformed static configuration. Hence, subsequent to the maneuver settling time t_s , the only energy-work exchange will be between the aerodynamic load terms and the actuator load term since there will be no change in the kinetic and elastic strain energies in the static post-maneuver settling period. The actuators will have to do work on the system to sustain the maneuver up until the termination time t_f of the steady maneuver state; but all of this work has to be transferred out from the system (net positive aerodynamic work) to the airstream.

Furthermore, certain actuator configurations such as distributed piezoelectric actuators, due to their nature cannot by themselves yield a generalized control load for the rigid-body coordinate displacement. Therefore, the rigid-body work through such an actuator system must always be equal to zero; the maneuver will be accomplished and sustained indirectly through the aerodynamic loads due to flexing of the surface by the non-trivial generalized flexible loads created by the control actuators. These results provide a tool for checking the accuracy of and gaining insight to the implementation of the aeroservoelastic solution.

9. OPTIMAL MODAL PERFORMANCE OUTPUT ALLOCATION

There are two quantities that are of importance in the control of elastic systems with distributed controls. From the control point of view, the control power required is of utmost importance and the least studied in the literature. The other quantity is the required strain energy from the structural point of view. Excessive control power expenditure and strain loading of the structure are not desirable. Both the control power and strain energy are positive definite and positive semi-definite quantities, respectively. They are also functions of the desired final state which is ultimately a synthesis of the modal states and the modal output performance that will be assigned to the modal controllers discussed above to achieve the maneuver. An important objective for the maneuver, therefore, would be to minimize a measure of control power and the strain energy required for the structure. To this end, we use a hybrid modal performance output allocation measure defined as:

$$POM = \alpha S_D + \beta U_{STR} \quad (43)$$

where POM is the modal performance output measure metric, K and 2 are positive semi-definite scalar

weightings and S_D is the transient modal or real control power, and U_{STR} is the elastic strain energy. Both of these quantities are ultimately functions of the assigned modal performance outputs z_r^* for the control design model. One can assign the elements z_r^* by posing the following **modal performance output allocation optimization problem**:

$$\text{Minimize } POM = \alpha S_D(z_r^*) + \beta U_{STR}(z_r^*)$$

Constraint:

$$\sum_{r=1}^{r=n_c} z_r^* = z^* \quad \forall \quad z(t_f) = -HA_{CL}^{-1}B_Z Z^* = z^* \quad (45)$$

where

$$2S_D = Z^{*T} B_Z^T A_{CL}^{-T} P A_{CL}^{-1} B_Z Z^* \quad 2U_{STR} = Z^{*T} B_Z^T A_{CL}^{-T} K_S A_{CL}^{-1} B_Z Z^* \quad P = P_M \vee P_R \quad (46)$$

z^* denotes the specified constraint value, that is, the desired maneuver output. The second form of the constraint in the above optimization problem can be posed in terms of the actual maneuver performance output $z(t_f)$ realized rather than the individual modal performance outputs z_r^* . This will insure that the desired output performance will be realized regardless of the approximations that may be inherent in the formulation and solution of the control problem and modal synthesis. One can even calculate the constraint for the evaluation model by using A_{CL-EVM} and B_{Z-EVM} in Eqs. (45, 46) for the evaluation model, and realize the desired maneuver performance level even in the presence of residual mode effects provided that the residual modes are stable; that is, A_{CL-EVM} is stable, which will have to be the case in order to realize the maneuver under any circumstances. The above poses a convex optimization problem for the unknowns z_r^* . Thus, having provided a rationale for also determining how to allocate the required modal performance outputs for the modal controllers, we close the solution of the aeroelastic maneuver problem and illustrate the approach.

10. ILLUSTRATION I: SHAPING OF A LIFTING SURFACE

We consider a cantilevered composite material plate model in an airstream which was studied both analytically and experimentally for aeroelastic and aeroservoelastic design purposes in the literature⁷⁻⁹. In regards to the latter purpose, the advantages of integrated aeroelastic structure-control design were demonstrated by simultaneous optimization of structural and control design parameters for maximizing the critical flight speed of the lifting surface. Full unsteady-aerodynamic effects were considered in Refs. (7,8). The plate has length $l = 0.305$ m, chord $c = 0.076$ m, and a thickness of 0.000804 m with a mass density of 1520 kg/m^3 ; other relevant data not presented in this report for brevity can be found in Refs. (7,8). The plate is dynamically modeled by a Ritz procedure using five assumed-mode shapes of uncoupled beam

bending and twist modes: 1st, 2nd bending (B), 1st, 2nd twist (T) and a parabolic chord-wise bending (CB) mode with associated coordinates as the generalized coordinates for the aeroelastic system. Since the plate is cantilevered no rigid-body coordinate exists and all coordinates represent flexible degrees of freedom. The particular plate configuration we consider here was the optimal configuration for the integrated design which had a maximum critical flight speed of 112.69 m/s (divergence) with an optimal active control system engaged with minimum control authority. To illustrate the approach presented in this report, the data for the above structure generated for a flight speed of 98.96 m/s at sea-level (corresponding to a 5784 N/m² = 0.84 psi dynamic pressure) was considered with the unsteady aerodynamics and aerodynamic inertia effects ignored. Structural damping of 0.15 was also added to each of the assumed modes. The undamped structural natural frequencies without aerodynamic effects were 61.13 (1 B), 320.02 (1 T), 407.3 (1 T & 2 B), 1214.10 (2 T), 2993.7 (CB) rad/s. The aeroelastic system has 10 modal-space-states with 5 pairs of complex conjugate eigenvalues with an unstable first aeroelastic mode. The aeroelastic eigenvalues are obtained as $2.3 \pm 61.3 i$, $-31.4 \pm 320.6 i$, $-1.5 \pm 405.1 i$, $-35.4 \pm 1213.7 i$, $-4.7 \pm 2993.3 i$ rad/s.

The maneuvering (set-point) objective is to twist the tip edge of the lifting surface by a slope which has a 1/4 chord length rise from the trailing edge to the leading edge, that is about a 14 degree twist of the wing-tip. The control system will warp the whole lifting surface to achieve this objective.

We consider a 4th order reduced-control design model which includes the first two aeroelastic system modes to achieve the maneuver, the first aeroelastic mode is unstable. Of the 0.25 slope that is to be achieved at the wing tip, we assign (without seeking optimum allocation) that $z_1^* = 0.03$ of this twist be achieved by warping the wing in its first aeroelastic mode and $z_2^* = 0.22$ of it be achieved by warping it in its second aeroelastic mode. These tasks are performed by independent modal controllers for the first and second aeroelastic modes, each employing a first-order modal compensator, essentially an integrator, on the modal-performance-output error feedback. The modal gains are computed for each modal-controller independently via eigenvalue allocation with uniform damping factors and the uncontrolled damped frequencies are not changed. The closed-loop eigenvalues were specified as: -30.0 , $-100.0 \pm 61.3 i$, and -30.0 , $-100.0 \pm 320.6 i$, for each modal controller including a first-order modal-compensator. As per Eq. (16) for both of the modal compensators, the following parameters were chosen $a_{cr} = 0.0001$, $b_{cr} = 1$, $k_{cr} = 0$ and $c_{cr} = 1$, $r = 1, 2$. The modal measurement matrices C_r were 2X2 identity matrices ($r = 1, 2$) resulting in a state-feedback design, and the modal-performance-output matrices are $h_1 = [-0.86 \quad 4.49]$ and $h_2 = [-21.46 \quad -12.30]$. The response of the synthesized DPCL-IMSC, which uses a spatially continuously distributed control field, is shown in Fig.(I-1) together with the response of the design-IMSC which ignores the modal coupling terms due to modal synthesis procedure. The wing tip achieves an angle-of-attack of 14 degrees at the end of about 0.2 sec of settling-time ($t_s=0.2s$). The warped steady-state wing shape is shown in Fig. (I-2) for this maneuver. Next, we attempt to duplicate this performance by a finite number of distributed local actuators.

We assume that a multitude of rectangular actuation domains are available for distributed actuation, each of which is size $0.1 l \times 0.25 c$ ($l = \text{span}$, $c = \text{chord}$) in the span-wise and chord-wise directions, respectively. The local control loading influence function associated with each actuator is normalized to non-dimensional unity, that is, $\psi_k(p) = 1$, $k=1,2,\dots,40$. The maneuver can be accomplished by a host of actuation profiles differing in number and locations, in particular 40 such actuators would cover the whole lifting

surface providing a 40 D.O.F's for control design, if desired. Certainly, any number of actuators can be utilized to partially cover the surface to achieve the maneuver. The particular perspective we use is essentially reminiscent of a finite-element-method for approximating a distributed-parameter-closed-loop control solution. The first actuation profile we demonstrate uses 6 actuators located on the edges of the surface starting at span-wise stations 0.5 l, 0.7 l and 0.9 l. The second actuation profile uses 20 actuators entirely covering the 1/2 of the surface outboard of the mid-span. The approximation solutions are obtained for both profiles via optimal approximation (OPAX) and Galerkin approximation (GALAX). The weighting parameters for the optimization in Eq.(39) were chosen as $\sigma = 0$, $\gamma = \gamma_p = 1$. Table 1 summarizes the resulting eigenvalues, power performances, F-norms of the modal gains G_M and the signal gains G , and the maximum and minimum steady-state control inputs required for the maneuver. The MATLAB optimization software was used to solve the optimization problem having 36 and 120 control gains as design variables for both actuation profiles. GALAX solution required mere SVD inversion. Note that for 6 actuators ($n_i = 6$) the OPAX and GALAX solutions have some control-spillover and therefore power-spillover to the uncontrolled modes. No appreciable spillover response is generated by such amount of spillover into uncontrolled high frequency modes, however, power is wasted. The 20-actuator solutions are practically identical to the DPCL-IMSC solution with almost no spillover. The DPCL-IMSC solution does not have any spillover by its nature. The maneuver responses, warped wing shapes of the approximations are essentially the same as those of the DPCL-IMSC as given in Figs. I-1 and I-2, and therefore are not shown. Note that the given signal strengths and gain figures are in natural pressure units for this problem and can be further converted to gains and signal strengths in other units relevant for a chosen actuator technology. No matter what that choice is, however, each actuator ultimately will have to provide the control action expressed by the units of this illustrative example.

11. ILLUSTRATION II: AEROSERVOELASTIC ROLL RATE -MANEUVERING OF A HIGH-SPEED AIR VEHICLE

The second illustrative example demonstrates roll-rate maneuvering of a high-speed (Mach 2) air vehicle for which a Finite Element Model (FEM) was developed at the AFRL/VASD Division. The original full set of mass, aerodynamic damping, aerodynamic stiffness and the structural stiffness matrices are available in terms of 1080 nodal degrees-of freedom of the FEM. The FEM is free to roll. However, for the particular illustration given here, we were provided the system matrices in terms 16 structural modal coordinates. Thus, the starting configuration-space EOM, Eq. (6) consists of 16 generalized coordinates which are these particular structural modal coordinates. The corresponding system matrices, therefore, are representations in terms of the particular structural (modal) configuration-space. Because the structural system is free to roll, the first generalized (structural modal) coordinate is the rigid body roll angle of the vehicle fixed reference frame and the remaining coordinates are the anti-symmetric flexible modal coordinates of the wing structure (a rigid fuselage was also assumed). We treat the resulting EOM in terms of the structural modal coordinates as the physical system and the evaluation model. The details of formulations of these matrices are given in Ref. (10) for a similar flight configuration. The system used here is for a different flight condition at a higher speed with modified structural parameters. No structural damping is included in the model, and we assume that for the given aerodynamic matrices a steady or quasi-steady aerodynamic model is permissible. It should be noted that the formulations we present in this report will remain valid even if more sophisticated unsteady aerodynamic models are to be used. However, in this case, additional algebraic

manipulations of the EOM would be needed together with aerodynamic state equations in order to cast the EOM into the form of Eqs. (6, 7). Such details are beyond the intended scope of the work, and our purpose here is to demonstrate the feasibility of the proposed modal synthesis approach to the maneuvering problem.

Aeroelastic Model: The flight dynamic pressure is 18.92 psi (130453.4 N/m², 1psi=6895 N/m²) at a flight speed of 24888 in/sec (2275.76 km/hr). There are 32 aeroelastic states corresponding to 16 DOF in the configuration-space, which consists of 16 structural modal coordinates. The solution of the aeroelastic eigenvalue problem is given in Appendix A, which is a computer generated output based on Matlab software. The first two aeroelastic eigenvalues are real and unstable with values of 0 and 2036.28 rad/sec; the first eigenvalue corresponds to a pure rigid-body displacement mode, the second eigenvalue corresponds to a hybrid velocity mode that includes rigid-body roll-rate and elastic velocities; however, it is dominated by the roll-rate. The remaining aeroelastic state-space modes are complex conjugate pairs with the conjugate pairs of aeroelastic modes 4, 6, 12, 16 being unstable. The rest of the 16 aeroelastic modes (32 state-space modes) are oscillatory and stable. Hence, all of these unstable modes must be controlled in order to achieve a desired roll-rate maneuver.

Aeroservoelastic solution: Since the rigid-body roll angle is not of interest, we do not control the first real simple mode corresponding to the first eigenvalue of "0"; however, we retain it as part of the first state-space modal dynamics in the control design and insure that no control input is generated on the corresponding modal equation. We accomplish this by assigning a zero weighting parameter for the corresponding modal state of the 0 eigenvalue simple mode in the quadratic modal-state weighting term of the LQR solution. If eigenvalue allocation (EVA) is used, we simply do not move the 0 eigenvalue. In computer simulation results, once the controls are designed, we move the uncontrolled "0" eigenvalue mode into the set of uncontrolled dynamics in the evaluation model as the first residual mode. Hence, the CDM has 6 modes, (modes 1, 2, 4, 6, 12, 16), 5 of which are conjugate pairs in the state-space, and the first mode consists of two simple unstable state-space modes (hence, also a pair); four pairs of the conjugate modes (1, 4, 6, 12, 16) are unstable in the uncontrolled configuration. Aeroelastic mode 2 is originally stable, since it is the lowest frequency mode in the set, it is included in the CDM to be a dominant performance mode which would require the least amount of effort to achieve the maneuver. With a first-order modal compensator augmented to each pair of state-space modes, the corresponding state-space for the CDM has 18 states. Without modal compensators, the CDM has 12 states. For simulation purposes, since the "0" eigenvalue simple mode is moved to the EVM set, the CDM has 17 and 11 states, respectively. The maneuver objective is to achieve a roll-rate of 1.57 rad/sec. The control design was done by using the LQR approach for each mode of the CDM independently and the generalized control loads for the DPCL-IMSC solution were synthesized from the design modal control inputs according to Eq. (12). Subsequently, a GALAX approximation of the DPCL solution was obtained for a chosen set of 14 actuators embedded in the wing structure. Appendix A presents the computer simulation results, and various control and system parameters used, most of which should be self-explanatory. We summarize the important results and observations below.

Distributed-parameter-control IMSC (DPCL-IMSC) solution: Although we design stabilizing controls for 6 modes, for this illustration, we allocate that the desired performance output of 1.57 rad/sec roll-rate be realized by the 2nd mode alone, that is, $z^* = z_r^* = 1.57$ rad/sec, while eliciting zero contribution in the

steady-state to the roll-rate from all other controlled modes. Furthermore, we hope that no performance degradation will occur due to residual modes. Figure(II-1) shows the simulation of the roll-rate for both the CDM and the EVMsimultaneously; the responses are identical. The maneuver is accomplished for the CDM and the EVM, that is there is no performance degradation even in the presence of full-order 32 state-space model of the 16 generalized coordinates. We note that in about 1.5 seconds, the roll-rate of 1.57 is achieved for the first generalized coordinate velocity, while the generalized velocities corresponding to all of the remaining elastic DOF practically vanish in the evaluation model (in a slightly longer simulation time all of the generalized flexible coordinate velocities become less than 1e-04).

The maximum steady-state modal control input required for the maneuver is (-747.65) on the 2nd aeroelastic mode, and the maximum steady-state generalized load is (- 4862.52 lbs or in-lbs) corresponding to the second generalized coordinate, which is the second structural mode of the FEM. Figure (II-2) shows the generalized loads required for the maneuver. The uncertainty of the units of this generalized load is due to lack of information we have on the units of the FEM data provided to us. Whatever the units are the level of required generalized load represents a realizable level. The generalized loads reported in Appendix A can be transformed to physical nodal loadings of the FEM according to the following expression

$$Q_{NODAL} = M_{FEM} E_{ns} Q \quad (47)$$

where M_{FEM} is the FEM mass matrix and E_{ns} is the structural modal matrix of the FEM corresponding to the ns structural modes taken as the generalized coordinates of the aeroelastic system. Because we did not have access to the FEM mass and structural modal matrices at this time, we could not generate the nodal control loads. However, if this step is carried out, one will generate control loads along every nodal DOF of the FEM; hence, the control solution is surrogate to a distributed-parameter-control solution exactly in the same sense that the FEM is the surrogate model of the distributed-parameter-structural system. Therefore, we refer to this solution as the distributed-parameter-closed-loop IMSC (DPCL-IMSC) solution.

The transient control power expended by the DPCL-IMSC is computed by solving the associated Lyapunov equation and is $S_D = 156.68KWatts = 210$ Horsepower (hp) = $1.39e+6$ in-lbs/sec. The total real control power through $t_f = 1.5$ secs of maneuvering is computed via integration as $S = 1586.59KWatts = 2127hp = 14.05 e+6$ in-lbs/sec. The Frobenius-norm (F-norm) of the power matrix P of the transient control power S_D is $5.12e+10$; and the F-norm of the modal gain matrix of the synthesized-IMSC solution is $1.12e+4$. These values should be compared below with the values for the GALAX approximation of this solution by a finite number of spatially-discrete axial load actuators imbedded in the rib elements of the wing structure.

Work-energy terms of the DPCL-IMSC solution are given with reference to the EVM, since there is no guarantee that these terms will balance for a CDM (unless all residual energy in the residual modes balance out). The total actuator energy that will be expended by the distributed-parameter-control (simulating a full nodal loading vector in the FEM as discussed above) is computed via integration to be 0.41WH (Watt-Hour) ($1.31e+4$ in-lbs) which is balanced by the work of all other effects computed as: 0.6WH ($1.91e+4$

in-lbs) for the elastic loads (energy is stored into the structure), $3.87e-5WH$ (1.23 in-lbs) for the kinetic energy which is almost exactly the rotational kinetic energy of the vehicle at the roll-rate of 1.57 rad/sec, $-0.25WH$ ($-7.97e+3$ in-lbs) for the aerodynamic damping work (energy is added to the structure by the aerodynamic rate terms), and $5.88e-2 WH$ ($1.87e+3$ in-lbs) for the aerodynamic stiffness work (energy is lost to the airstream from the structure). We should note the very low levels of work-energy terms associated with the DPCL-IMSC solution. Also we note that in this illustration, the aerodynamic damping term works with the actuators to add as much energy as $(2.5/4.1 = 61\%)$ of the actuator energy to shape the wings storing $1/3$ of the required elastic energy to the wings. However, with the exception of elastic and kinetic energies, energy quantities are sign-variant and can be misleading from the control perspective; therefore they do not indicate the intensity of control activity demanded of the actuators, which is more realistically expressed by the positive-definite control power terms. For this particular illustration, the steady-state configuration is achieved in about less than $t_s = 2$ seconds. Subsequent to this, there will be no more changes in the elastic and kinetic energy levels hence all work-energy exchange will occur between the actuators and the aerodynamic terms to nullify each other, whatever the actuators put in will be shed into the air stream, due to the achieved wing shape, through the aerodynamic stiffness work. This observation has been verified through computer simulations.

Inspection of the work-energy terms decomposed as rigid-body and flexible motion terms reveals more information. The kinetic energy is imparted to the vehicle totally by the actuators, and the aerodynamic damping and stiffness work terms nullify each other through the rigid-body roll motion. On the other hand, no kinetic energy is generated through the flexible motion, and all of the elastic energy stored into the wings is provided by the actuators and the aerodynamic damping and stiffness terms. The aerodynamic stiffness term due to elastic deformation creates a net opposing roll moment and extracts energy from the vehicle through the rigid-body motion (it extracts part of the actuator energy added and all of the energy added by the aerodynamic damping term); whereas the generalized elastic loads generated by this term add energy to the structure through elastic displacements. In comparison, the aerodynamic damping loads due to roll-rate add energy to the vehicle through the rigid-body motion (all of which is extracted by the aerodynamic stiffness work), and to the elastic structure through flexible deformations. We must note that these observations via simulations are based on the aerodynamic data (which was generated at the AFRL/VASD by using the ASTROS software package) that we were provided for this illustration. Whether these observations are consistent with the realistic observable aerodynamic phenomena or whether the aerodynamic models employed are of high-fidelity is another matter. Such issues would not have any consequences for the control design method that is proposed in this report, albeit numbers and observations may be altered with different aeroelastic models.

GALAX approximation to the DPCL-IMSC solution: the DPCL-IMSC aeroservoelastic solution presented and discussed above is attempted for implementation by a finite-number of multitude of axial load actuators imbedded in the elements of the ribs stationed along the wing span. For illustration purposes we considered 14 such actuators on each wing (actuators 13 - 22, and 37- 40) the first ten of which are nominally located in the wing ribs near the mid-span, the last 4 of which are located at the wing tip. The simulation results are again given in Appendix A under the headings of "GALAX" wherever appropriate. Because the given actuator set represents an internal loading set (action-reaction in the axial-force rib members), no net external roll- moment can be generated directly by these actuators. This is in contrast to

the DPCL-IMSC solution which yields a necessary control load distribution, and therefore does not preclude generation of roll- moments or external out-of-plane loads on the flexible structure. Hence , the chosen actuator set is constrained from the beginning relative to the DPCL-IMSC solution; nevertheless we attempt to have these actuators mimic the DPCL-IMSC solution as best as they can by using the approximation techniques presented in Sec. 7.

The given actuators realize exactly the response of the DPCL-IMSC solution in the CDM and accomplish the roll-rate of 1.57 rad/sec as presented in Fig. (II-1). The CDM of the GALAX solution has the same eigenvalue spectrum as the DPCL- IMSC solution. In the EVM simulation shown in Fig. (II-3), we note that there does not appear to be significant degradation of the desired maneuver rate with the exception of the oscillatory ripples superposed on the desired roll-rate behavior. The ripples are due to residual mode excitation in the EVM. Although the response appears to be satisfactory, the power, work-energy and control gains and control loads required to obtain this maneuver profile tell a different story. We note that in the GALAX solution we obtain the physical control loads since we were provided the complete actuator profile, the D matrix, by the AFRL/VASD.

The maximum steady-state modal control load is (-3919.37) on the 10th aeroelastic mode (12th mode in the modes rearranged for control), and the maximum steady-state generalized control load is (119,151.42 lbs or in-lbs) on the 11th generalized coordinate (the DPCL solution yields a load of 6.06 for the same coordinate). The generalized loads for the GALAX actuator set shown in Fig. (II-4) are in general 3 or 4 orders of magnitude higher than the DPCL loads for the same generalized coordinates. The maximum physical actuator load is (9.16e+6 lbs) and occurs at actuator number 16 (4th in the computer output), all other actuators require similar order of magnitude of physical control loads as shown in Fig. (II-5). These control load levels are clearly infeasible. For the DPCL solution, we could not generate the physical control loads at the nodes of the FEM due to lack of the necessary FEM data. However, one can surmise by comparison that the DPCL nodal loads (which can be considered as discrete-physical loads) would similarly be 3 or 4 orders of magnitude lower than the GALAX solution, well within realizable limits.

The transient modal control power levels of the GALAX solution, obtained for the CDM, by definition, are almost identical to the real control power levels of the DPCL solution (for the DPCL-IMSC solution real and modal control powers are identical and there is no control power spillover by the nature of the solution). This is to be, since the performance of the CDM of the GALAX solution is designed to have an eigenvalue spectrum identical to the CDM of the DPCL -IMSC solution. However, the real control powers of the GALAX solution are $S_R = 1.89e+6KW = 2.53e+6hp$, and $S_{RD} = 1.85e+5 = 2.48e+5 hp$ for the total and transient powers, respectively. These are three orders of magnitude higher than those of the DPCL solution and again represent infeasible control power levels. The F-norm of the modal power matrix P_M of the transient modal control power S_{MD} is $5.12e+10$; and the F-norm of the modal gain matrix G_M of the GALAX solution is $1.12e+4$ which are identical to those of the DPCL solution. But the F-norm of the real power matrix P_R of the transient real control power S_{RD} is $9.08e+13$, and the F-norm of the real control gain matrix G is $6.82e+9$. These figures reflect that there is unreasonably high-levels of control power spillover in the GALAX actuator set which is the price one may pay for discretizing a control actuation profile if not done properly. The fact that there is not a significant response degradation in the EVM simulation of the GALAX solution in Fig. (II-3) is no point of comfort, but a point of distress indeed. This is in keeping with

our long-held observation that there is more to it than meets the eye in the simulation of control of flexible systems; the chosen actuator profile simply wastes enormous amount of control power and needs to be reconsidered for power efficient control. We note that at the end of final time of maneuver the elastic generalized velocities do not vanish in the GALAX EVM indicating the effects of control-spillover.

As for the **work-energy terms of the GALAX solution**, we make the following brief observations from the EVM results. Again the work-energy balance is verified by the 4.85WH (1.55e+5 in-lbs) of actuator work on the right-hand side and the same amount of total work on the left-hand-side due to 5.38WH (1.72e+5 in-lbs) of elastic energy, 9.85e-4 WH (31.36 in-lbs) of kinetic energy, - 0.29WH (- 9.14e+3 in-lbs) of aerodynamic damping work, and - 0.25 WH (-7.90 e+3 in-lbs) of aerodynamic stiffness work. In comparison to the DPCL solution, we note that in the GALAX solution the actuators do about 10 times more work and about 10 times more elastic energy is stored due to residual mode excitation. For the same reason, the kinetic energy includes elastic kinetic energy due to residual mode rates. We note that the elastic energy is provided by the actuators and both of the aerodynamic work terms. Since the actuators are internal axial elements, the given actuator set does no work through the rigid-body vehicle motion as was conjectured previously. The kinetic energy is about 1.23 in-lbs, which is due to the rigid-body roll -rate, and the aerodynamic work terms nullify each other to within (-1.23 in-lbs) which leaves the desired roll-rate kinetic energy (damping term adds, stiffness term extracts energy) through the rigid-body displacement. In fact, since the given actuator set cannot generate a rigid-body generalized load (a rolling-moment), aerodynamic load terms are the only mechanism by which the desired maneuver can be accomplished; the given actuator set deforms the wing to alter the aerodynamics to produce a rolling- moment on the rigid-body coordinate. All of the actuator work is done through flexible displacements, and likewise both aerodynamic terms add energy to the system resulting in elastic energy storage (along with the actuators) and an increase in the kinetic energy through residual elastic displacements.

From the above results and comparison of the GALAX and DPCL solutions we conclude that the given actuator profile constitutes a poor set although we have not tried very hard to identify the best actuator configuration for the given data. Based on a several other simulations, we believe that the results would not change significantly. Whereas the DPCL-IMSC solution indicates that the desired maneuver can be performed by means of feasible levels of control power, gain, energy and load; the problem of finding discrete actuator sets that perform with comparable level of figures presents itself as another task. For the same reason, we do not present results to demonstrate an OPAX solution to this problem. Furthermore, our initial attempts for an OPAX solution proved to be beyond the limits of the Matlab optimization software which we had successfully used for the composite-plate illustration above. The failure of the Matlab software also stems from the numerical conditioning of the actuator profile matrix which does not appear to be a "wholesome" set based on our experience with the GALAX solution.

Finally, in concluding this illustration, we report in Appendix B the computer results for the same problem in which the performance output allocation to the modal controllers is optimized by selecting three of the CDM modes to be the performance modes, namely, modes 1, 2, and 6. In the performance mode optimization problem, we minimize a hybrid measure of the transient control-power and the elastic strain energy stored in the structure. We leave it to the reader to interpret these results much in the same fashion as we have done above.

12. CONCLUSION

A number of new features for the modal study of aeroelastic systems are introduced in this work. A unique modal formulation of the aeroelastic system is given in terms of real conjugate modal matrices and modal-states. Bi-orthonormality relationships are established both with respect to the aeroelastic system matrices and the structural matrices. Distributed actuation control of the aeroelastic system via the IMSC technique is introduced, specifically for maneuver set-point control, and the globally optimal distributed-parameter-closed-loop-control (DPCL-IMSC) is formulated by modal synthesis. Control power expressions for the non-self-adjoint aeroelastic system are given as extensions of previous definitions for a self-adjoint elastic system. Implementation of the DPCL-IMSC solution by means of distributed, spatially-discrete actuation profiles is addressed through an optimal gain distribution approximation problem which incorporates transient response and power expenditure trade-off. A Galerkin approximation is also given for the same purpose. The optimal approximation approach has no restriction on the number of actuators, whereas the Galerkin approximation has a minimum number requirement. The work-energy terms due to elastic, kinetic, aerodynamic and actuator loads are given for an aeroelastic system. A modal performance output allocation optimization problem is also defined, which minimizes a hybrid measure of transient control power and elastic strain energy of the structure during the maneuver. The modal synthesis approach is first illustrated for shaping a lifting surface simulated by a composite plate by using distributed actuation to achieve a maneuver set-point, a prescribed angle of attack for the wing tip. The approach is also illustrated for a realistic wing configuration at Mach 2 for a specified roll-rate maneuver, and the distributed-parameter-control equivalent control power, generalized control loads, control gains and the work-energy requirements are studied. The results indicate that the requirement levels are and may be feasible for an effectively distributed-parameter-control equivalent actuator profile. However, the results also indicate that an unsatisfactory configuration of spatially-discrete actuators would require infeasible levels of control loads, control gains, and control-power to mimic the distributed-parameter-control equivalent maneuver response. In this case, the residual mode interactions through poor actuator configurations for the control task play an important role in driving the requirement levels to infeasible values. Further studies would be required to identify discrete actuator configurations and even aerodynamic parameters, in conjunction with a known distributed-parameter-control actuation profile solution, via an interdisciplinary approach that can accomplish the maneuver within physically realizable control power, control gains, energy and control forces comparable to the feasible levels of the distributed-parameter-control solution.

13. ACKNOWLEDGMENT

This work was supported by Air Force Research Laboratory, Air Vehicle Directorate, AFRL/VASD, WPAFB, Ohio under the CSA Prime Contract F33615-94-C-3200 "Aerospace Structures Information and Analysis Center"; Subcontract 3413.39/00.

14. REFERENCES

1. H. Öz, "Distributed modal-space control and estimation with electroelastic applications", *Structronic Systems: Smart Structures, Devices and System: Systems and Control*, Editors: H.S. Tzou, A. Guran, U. Gabbert, J. Tani, E. Breitbach, Volume 2, Series on Stability, Vibration and Control of Systems, pp. 179-262, World Scientific Publishers, Singapore, 1997.
2. H. Öz, K. Farag, and V. B. Venkayya, "Efficiency of Structure-Control Systems", *Journal of Guidance Control and Dynamics*, Vol. 12, No. 3, pp.545-554, 1990.
3. H. Öz, "Efficiency modes analysis of structure-control systems" *Journal of Guidance, Control and Dynamics*, Vol.17, No. 5, pp. 1028-1036, 1994.
4. H. Öz, "Independent Modal-Space Control and Estimation with distributed piezoelectric actuators and sensors" *3rd SPIE Smart Structures Conference, Mathematics and Control in Smart Structures*, Vol. 2715, pp.196-207,1996.
5. H. S. Tzou, and J. J. Hollkamp, "Collocated Independent Modal Control with self-sensing orthogonal piezoelectric actuators (Theory and Experiment) ", *Smart Materials and Structures*, Vol. 3, No.3, pp.277-284, 1994.
6. H. Öz, " Optimal Approximations to Distributed-Parameter-Closed-Loop Structures", AIAA Paper No:93-1656, *Proceedings of the 34th Structures, Structural Dynamics and Materials Conference*, pp. 3096-3107, 1993.
7. T. N. Dracopoulos, and H. Öz , "Integrated aeroelastic control optimization of laminated lifting surfaces", *Journal of Aircraft*, Vol.29, No: 2, pp. 280-288, 1992.
8. T. N. Dracopoulos, *Aeroleastic control of composite lifting surfaces -- integrated aeroelastic control optimization*, Ph.D. Dissertation, Aerospace Engineering, The Ohio State University, Columbus, 1988.
9. S. J. Hollowell, and J. Dugundji, "Aeroelastic flutter and divergence of stiffness coupled, graphite/epoxy cantilevered plates", *Journal of Aircraft*, Vol. 21, pp. 69-76, 1984.
10. N. S. Khot, "Deformation of a flexible wing using an actuator system for a rolling maneuver without ailerons", AIAA Paper presented at the SDM Meeting, *Proceedings of the 39th Structures, Structural Dynamics and Materials Conference*, Long Beach, Ca., April 1998.

TABLE: 1 PROPERTIES OF DPCL-IMSC AND ITS OPAX AND GALAX APPROXIMATIONS VIA DISTRIBUTED ACTUATION FOR THE COMPOSITE-PLATE LIFTING SURFACE

	DPCL-IMSC	OPAX 6 actuators	OPAX 20 actuators	GALAX 6 actuators	GALAX 20 actuators
Closed-loop Eigenvalues	-100.0 ± 61.3 i -100.0 ± 320.6 i -30.0, -30.0	-100.08 ± 61.15 i -99.99 ± 320.63 i -30.01 ± 0.10 i	-100.08 ± 61.15 i -99.92 ± 320.68 i -30.02 ± 0.00 i	-100.08 ± 61.15 i -99.92 ± 320.68 i -30.01 ± 0.24 i	-100.08 ± 61.15 i -99.92 ± 320.68 i -30.01 ± 0.24 i
S_R	202.18W	208.02W	208.02W	324.46W	209.25W
S_M	202.18W	203.27W	203.27W	208.02W	208.02W
S_{RD}	24.47W	25.04W	25.04W	37.29W	25.19W
S_{MD}	24.47W	24.47W	24.47W	25.04W	25.04W
Max / Min steady-state control signal	$f_{z2}^M = -2.48$ $f_{z1}^M = -0.05$ (m / s ²)	$F_4 = 11876.82$ $F_2 = -3940$ (N / m ²)	$F_2 = 1214.51$ $F_{10} = 34.85$ (N / m ²)	$F_2 = 4048.54$ $F_3 = -839.47$ (N / m ²)	$F_9 = -1164.39$ $F_{15} = -21.37$ (N / m ²)
Modal G_{MF} Signal G_F	1587.94 439.18	1589.66 1.07 e+7	1589.66 9.52 e+5	1589.64 2.35 e+6	1589.64 9.5 e+5

FIG.I-1: DESIGN-IMSC(--), DPCL-IMSC(-), PERFORMANCE OUTPUT

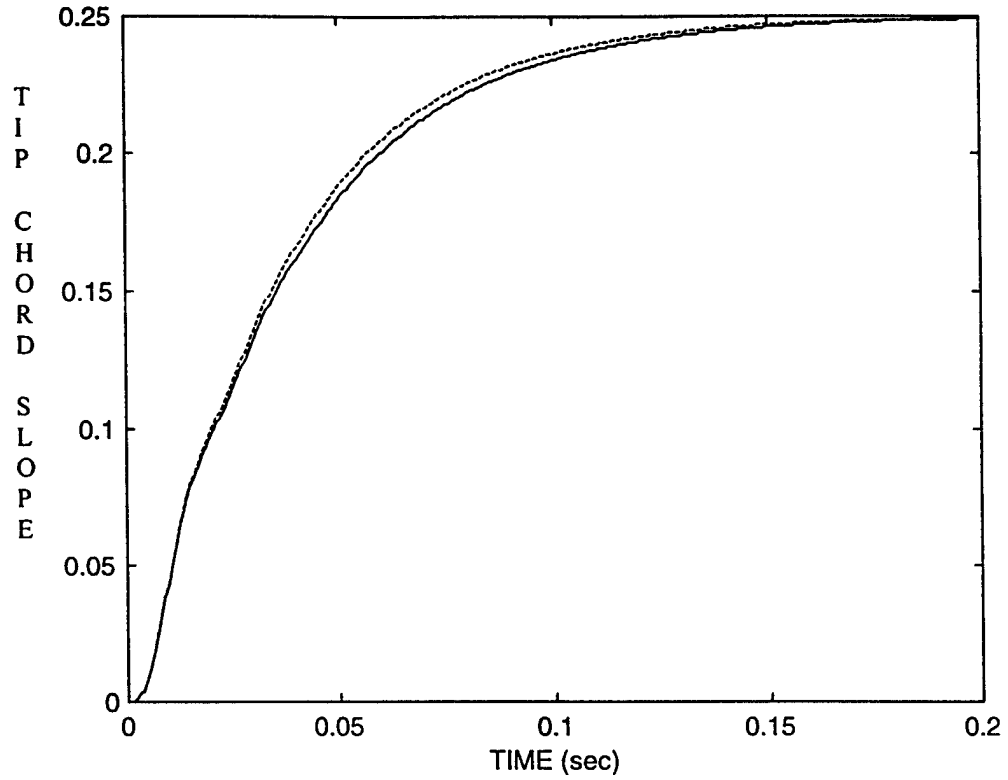


FIG.I-2 DPCL-IMSC DEFORMED WING SURFACE (mm)

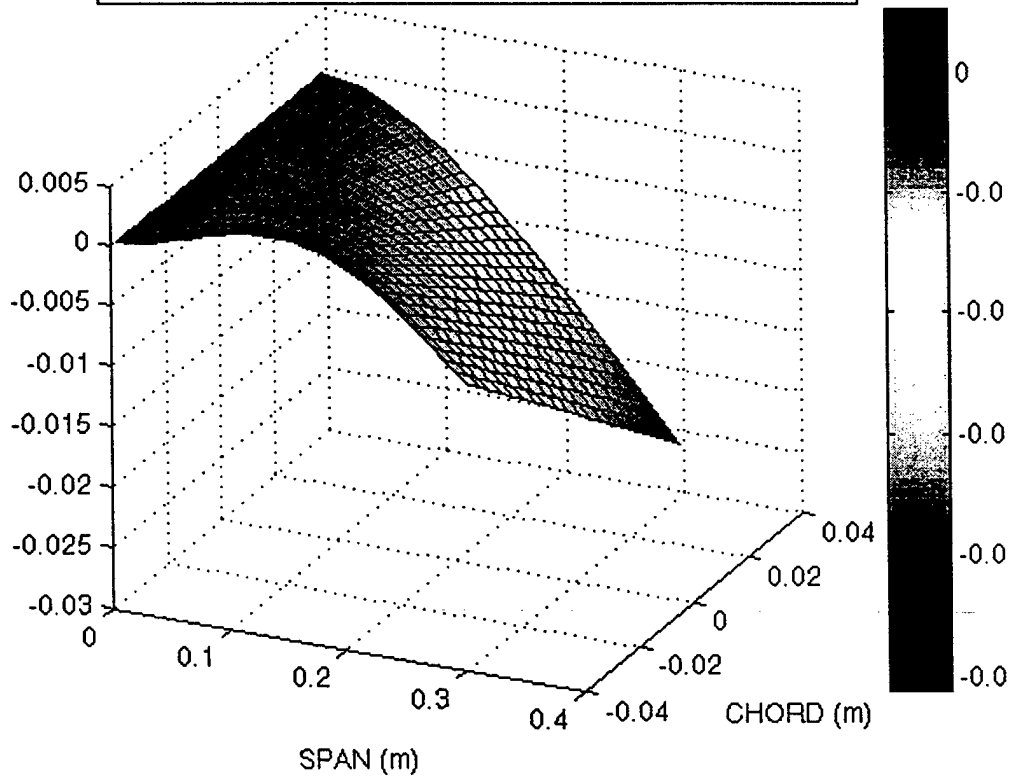


FIG.II-1: DPCL (CDM and EVM) AND GALAX-IMSC (CDM) PERFORMANCE OUTPUT (Rad/Sec)

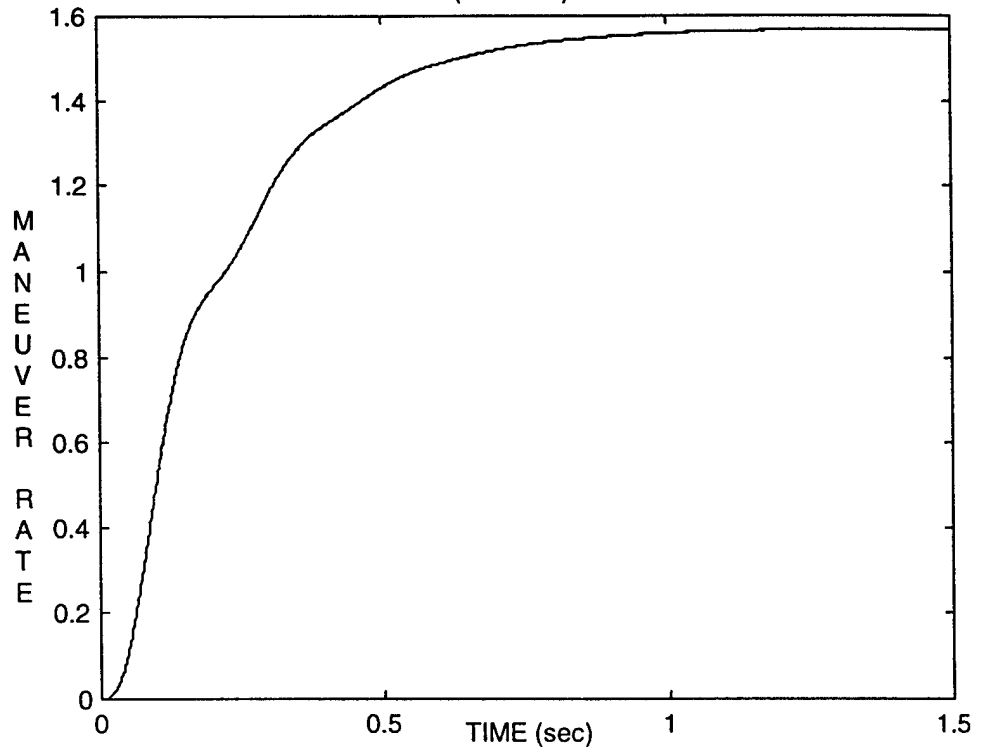


FIG.II- 2: DPCL-IMSC GENERALIZED CONTROL LOADS (lbs or in-lbs)

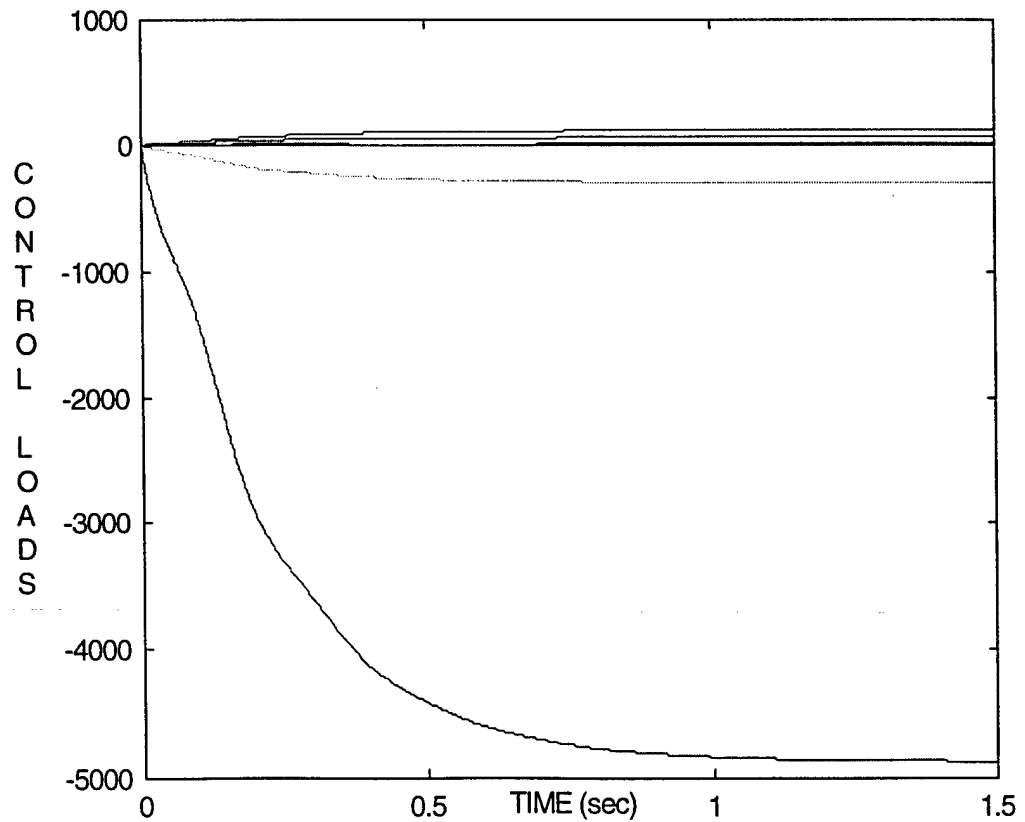


FIG.II-3: DPCL AND GALAX-IMSC(ripples), EVM PERFORMANCE OUTPUT (Rad/Sec)

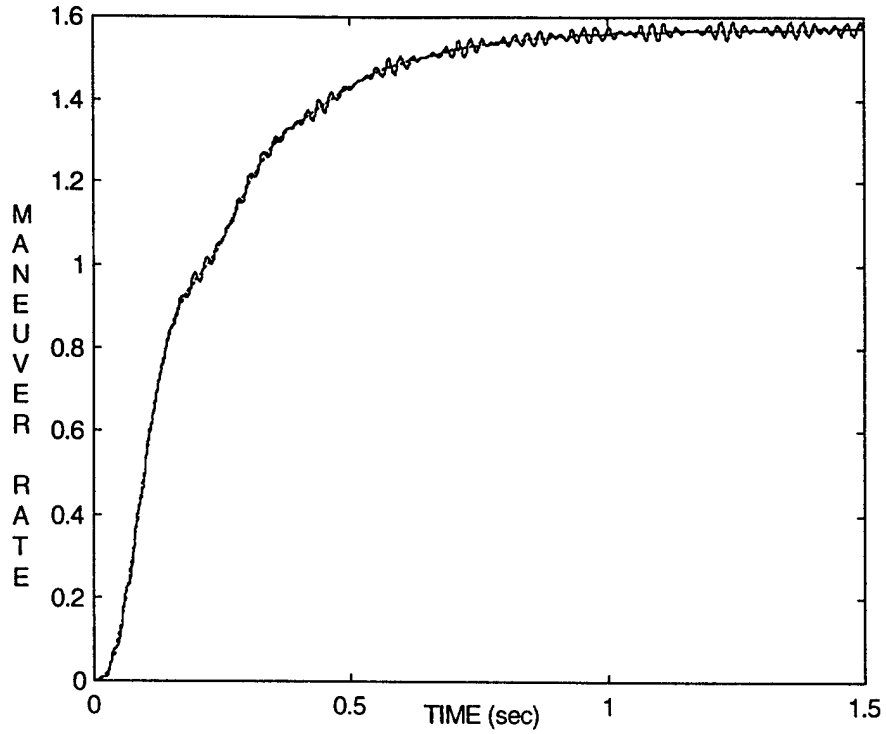


FIG. II-4: GALAX-IMSC GENERALIZED CONTROL LOADS (lbs or in-lbs)

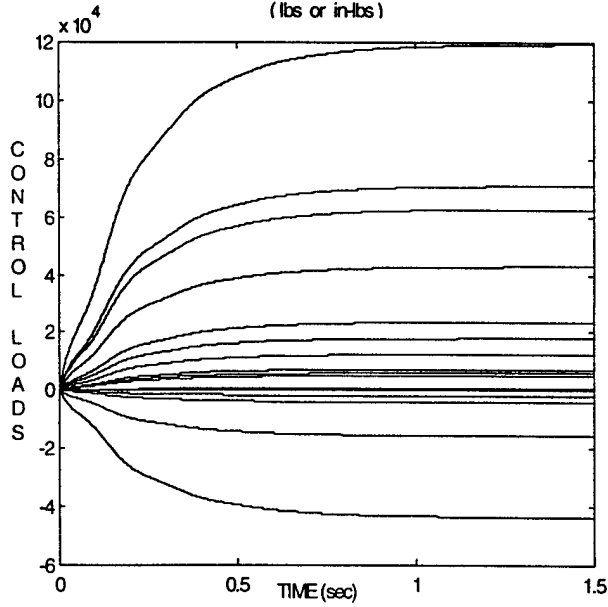
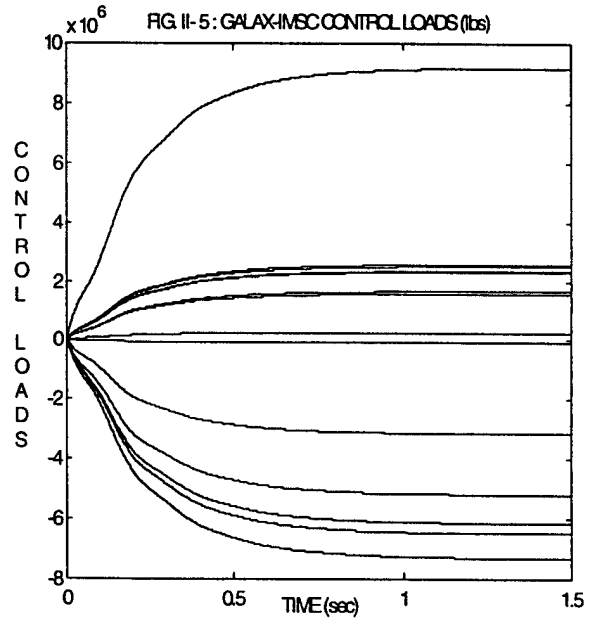


FIG. II-5: GALAX-IMSC CONTROL LOADS (lbs)



APPENDIX A : DPCL-IMSC AND GALAX-IMSC COMPUTER RESULTS FOR HIGH-SPEED WING

```
#####
MATLAB PROGRAM FOR AEROSERVOELASTIC MANEUVER VIA MODAL SYNTHESIS
#####
```

```
*****
AEROELASTIC MODAL ANALYSIS AND DISTRIBUTED-PARAMETER MODAL CONTROL VIA IMSC
*****
```

-- The units are {inches, pound-force and seconds} unless noted otherwise --

Air density (slug/ft³) : 0.001267
 Flight Speed : 24888 in/sec 2275.7587 km/hr
 DYNAMIC PRESSURE (psi): 18.9235

 Aeroelastic Eigenvalues (rad/sec or 1/sec)

Real Part	Imaginary Part
3.85581e-012	-9.16743e-016
2.03628e+003	8.77400e-014
-6.66482e-003	3.02105e+001
-6.66482e-003	-3.02105e+001
-8.69003e+000	8.63252e+001
-8.69003e+000	-8.63252e+001
7.65623e+000	8.65307e+001
7.65623e+000	-8.65307e+001
-1.04895e-003	1.23540e+002
-1.04895e-003	-1.23540e+002
5.11588e+000	1.50083e+002
5.11588e+000	-1.50083e+002
-5.24335e+000	1.50347e+002
-5.24335e+000	-1.50347e+002
-2.61625e-002	2.32295e+002
-2.61625e-002	-2.32295e+002
-1.76546e-002	2.80759e+002
-1.76546e-002	-2.80759e+002
-6.65399e-004	2.86147e+002
-6.65399e-004	-2.86147e+002
-5.03253e-002	3.18735e+002
-5.03253e-002	-3.18735e+002
5.12004e-003	3.43830e+002
5.12004e-003	-3.43830e+002
-3.16203e-002	4.26258e+002

-3.16203e-002	-4.26258e+002
-1.96150e-003	4.62506e+002
-1.96150e-003	-4.62506e+002
-3.28350e-001	4.76166e+002
-3.28350e-001	-4.76166e+002
3.31144e-001	4.94864e+002
3.31144e-001	-4.94864e+002

Modes Selected (modsel) for Control-Design-Model (wrt the order above)

1 2 4 6 12 16

Modal Control-Design Methods (selections below are wrt the modsel):

... LQR(Linear Quadratic Regulator) Design is used ...

The LQR weighting matrices for Modal Controllers

State Weightings | Compensator State Weightings | Control Weightings

1.00000e+000	1.00000e+002	1.00000e-004

!!!Modal Compensators ARE implemented!!!

Compensator matrices for Modal Controllers

ac	bc	gc	kc
-1.00000e-004	1.00000e+000	1.00000e+000	0.00000e+000
-1.00000e-004	1.00000e+000	1.00000e+000	0.00000e+000
-1.00000e-004	1.00000e+000	1.00000e+000	0.00000e+000
-1.00000e-004	1.00000e+000	1.00000e+000	0.00000e+000
-1.00000e-004	1.00000e+000	1.00000e+000	0.00000e+000
-1.00000e-004	1.00000e+000	1.00000e+000	0.00000e+000

NON-PISAS means composite compensator and modal dynamics,
All gains are designed by either LQR or EVA

NON-PISAS Modes: 1 2 3 4 5 6

Method for Modal Synthesis of the Distributed-Parameter Control is: METHOD=1

Aeroservoelastic Closed-Loop Eigenvalues of the Control-Design-Model

***** DESIGN-IMSC ***** SYNTHESIZED-IMSC *****

(rad/sec or 1/sec):			
Real Part	Imaginary Part	Real Part	Imaginary Part
-2.04980e+003	0.00000e+000	-2.04980e+003	0.00000e+000
-1.14638e+000	0.00000e+000	-1.07584e+001	4.94965e+002
-8.71524e+000	3.16349e+001	-1.07584e+001	-4.94965e+002
-8.71524e+000	-3.16349e+001	-5.24078e+000	3.43867e+002
-4.92715e+000	0.00000e+000	-5.24078e+000	-3.43867e+002
-1.82064e+001	8.53780e+001	-7.36541e+000	1.49992e+002
-1.82064e+001	-8.53780e+001	-7.36541e+000	-1.49992e+002
-1.32155e+000	0.00000e+000	-1.82064e+001	8.53780e+001
-7.36541e+000	1.49992e+002	-1.82064e+001	-8.53780e+001
-7.36541e+000	-1.49992e+002	-8.71524e+000	3.16349e+001
-6.82840e-002	0.00000e+000	-8.71524e+000	-3.16349e+001
-5.24078e+000	3.43867e+002	-4.92714e+000	0.00000e+000
-5.24078e+000	-3.43867e+002	-1.14638e+000	0.00000e+000
-2.99871e-001	0.00000e+000	-1.32156e+000	0.00000e+000
-1.07584e+001	4.94965e+002	-6.82796e-002	0.00000e+000
-1.07584e+001	-4.94965e+002	-4.19364e-001	0.00000e+000
-4.19365e-001	0.00000e+000	-2.99874e-001	0.00000e+000

=====

IMSC Apparent Transient Modal Power and Gain Norms

=====

Design-IMSC:

Fro(Power)	Trace(Power)	Fro(Modal Gain)
1.45479e+008	1.67784e+008	1.12372e+004

Synthesized-IMSC:

Fro(Power)	Trace(Power)	Fro(Modal Gain)
1.45479e+008	1.67786e+008	1.12385e+004

IMSC True Transient Modal Power Norms

=====

Synthesized-IMSC		Design-IMSC	
Fro(Power)	Trace(Power)	Fro(Power)	Trace(Power)
5.11708e+010	5.88578e+010	5.12000e+010	5.76813e+010
Alternate calculation			
5.11708e+010	5.88578e+010		

 OPTIMUM APPROXIMATIONS TO THE DISTRIBUTED-PARAMETER IMSC CONTROL (DPCL-IMSC)
 BY USING SPATIALLY-DISCRETE DISTRIBUTED CONTROL PROFILES
 #####

 GALERKIN APPROXIMATION

NUMBER OF MODES CONTROLLED: 6 NUMBER OF INPUTS: 14

Selected actuator Configuration:

Columns 1 through 12

13 14 15 16 17 18 19 20 21 22 37 38

Columns 13 through 14

39 40

 Aeroservoelastic Closed-Loop Eigenvalues of the Control-Design-Model
 via Galerkin Approximation

*****BASED ON DESIGN-IMSC ***** BASED ON SYNTHESIZED-IMSC *****

rad/sec or 1/sec):			
Real Part	Imaginary Part	Real Part	Imaginary Part
-2.04980e+003	0.00000e+000	-2.04980e+003	0.00000e+000
-1.07584e+001	4.94965e+002	-1.07584e+001	4.94965e+002
-1.07584e+001	-4.94965e+002	-1.07584e+001	-4.94965e+002
-5.24078e+000	3.43867e+002	-5.24078e+000	3.43867e+002

-5.24078e+000	-3.43867e+002	-5.24078e+000	-3.43867e+002
-7.36541e+000	1.49992e+002	-7.36541e+000	1.49992e+002
-7.36541e+000	-1.49992e+002	-7.36541e+000	-1.49992e+002
-1.82064e+001	8.53780e+001	-1.82064e+001	8.53780e+001
-1.82064e+001	-8.53780e+001	-1.82064e+001	-8.53780e+001
-8.71524e+000	3.16349e+001	-8.71524e+000	3.16349e+001
-8.71524e+000	-3.16349e+001	-8.71524e+000	-3.16349e+001
-1.14638e+000	0.00000e+000	-4.92714e+000	0.00000e+000
-4.92715e+000	0.00000e+000	-1.14638e+000	0.00000e+000
-1.32155e+000	0.00000e+000	-1.32156e+000	0.00000e+000
-6.82840e-002	0.00000e+000	-6.82796e-002	0.00000e+000
-4.19365e-001	0.00000e+000	-4.19364e-001	0.00000e+000
-2.99871e-001	0.00000e+000	-2.99874e-001	0.00000e+000

GALAX-IMSC Transient Power and Gain Norms
=====

Design-IMSC (stated for reference):

```
-----
Fro(Power)          Trace(Power)          Fro(Modal Gain)
1.45479e+008        1.67784e+008        1.12372e+004
```

Galax based on Design-IMSC:

```
-----
Fro(ModalPower)    Trace(ModalPower)    Fro(ModalGain)
5.12000e+010       5.76813e+010       1.12372e+004
Fro(RealPower)     Trace(RealPower)     Fro(RealGain)
9.08225e+013       9.58044e+013       6.81913e+009
```

Galax based on Synthesized-IMSC:

```
-----
Fro(ModalPower)    Trace(ModalPower)    Fro(ModalGain)
5.12006e+010       5.76832e+010       1.12385e+004
Fro(RealPower)     Trace(RealPower)     Fro(RealGain)
7.87001e+013       8.36496e+013       6.73475e+009
```

```
#####
SIMULATIONS, CONTROL POWER AND ENERGY-WORK QUANTITIES:
#####
```

Output Performance Allocation: Do you want to optimize?

Enter 1 to optimize, enter 0 for user assignment : 0

Desired Maneuver Rate (rad/sec): 1.57

enter number of performance modes
(must not exceed the number of controlled modes): 1

Select the performance modes (wrt the order in modsel)
 [row vector(include the brackets as shown)] : [2]
 Output Performance ratio in % for mode : 2 100 % left
 enter performance ratio in % for the mode : 100

Commanded Reference is: 1.57

Specified Commanded Reference Allocation for Modal Controllers:

0.00000 1.57000 0.00000 0.00000 0.00000 0.00000

Allocation sum (must be equal to Commanded Reference): 1.57

Specified % Output Performance Allocation for Modal Controllers:

0.00000 100.00000 0.00000 0.00000 0.00000 0.00000

Allocation sum (must be equal to 100%): 100

Do you want Control Model Simulation?
 enter 1(yes) or 0 (no)) :1

Final Output Value (Maneuver Rate) for Control-Design-Model

 Design-IMSC: 1.57 Synthesized DPCL-IMSC: 1.57

Final Values of Control Inputs:

 Design-IMSC(modal) | Syn. DPCL-IMSC(modal) | Syn. DPCL-IMSC(generalized)

0.000000000e+000	-3.111166375e-015	7.214485475e-001
-7.476525407e+002	-7.476526637e+002	-4.862517590e+003
-2.700895852e+002	-2.700892496e+002	1.185228946e+002
0.000000000e+000	2.845134060e-001	-3.083120450e+002
0.000000000e+000	-8.487943504e-001	-5.658394602e+000
0.000000000e+000	-2.074230215e+000	4.466912997e+001
0.000000000e+000	-3.593678804e+000	9.868231204e+001
0.000000000e+000	7.858741267e-004	2.947969290e-001

0.000000000e+000	-1.185607200e-002	-3.091698676e+000
0.000000000e+000	2.989456948e-003	1.329872047e+001
0.000000000e+000	6.513289653e-002	6.060742534e+000
0.000000000e+000	1.571523718e+000	-5.073508719e+000
0.000000000e+000	-5.115261467e-001	7.256734231e+000
0.000000000e+000	2.986622915e-010	8.434519916e-001
0.000000000e+000	3.740487740e-002	5.479784590e+000
0.000000000e+000	5.683090319e-012	6.830620640e+000
0.000000000e+000	-4.084354739e+000	0.000000000e+000
0.000000000e+000	2.769462474e-010	0.000000000e+000
0.000000000e+000	6.967366641e-002	0.000000000e+000
0.000000000e+000	-4.092277208e-011	0.000000000e+000
0.000000000e+000	-3.929098561e-002	0.000000000e+000
0.000000000e+000	1.475268025e-010	0.000000000e+000
0.000000000e+000	4.491718222e-002	0.000000000e+000
0.000000000e+000	-2.859209150e-010	0.000000000e+000
0.000000000e+000	-4.399418004e-001	0.000000000e+000
0.000000000e+000	-6.660185453e-011	0.000000000e+000
0.000000000e+000	-1.248584462e-002	0.000000000e+000
0.000000000e+000	9.767218631e-011	0.000000000e+000
0.000000000e+000	4.339406960e-003	0.000000000e+000
0.000000000e+000	-2.644692370e-010	0.000000000e+000
0.000000000e+000	-2.570921866e-002	0.000000000e+000
0.000000000e+000	4.252527638e-010	0.000000000e+000

~~~~~  
ENERGY-WORK FOR IMSC-SYNTHESIZED DISTRIBUTED-PARAMETER CONTROL  
(CDM = Control-Design-Model)  
~~~~~

Final Generalized Velocities	Final Generalized Displacements
=====	
1.5690	0.0003
-0.0203	-5.3373
0.0228	0.1311
0.0515	-0.3291
0.0033	-0.0052
0.0269	0.0134
-0.0229	0.0642
-0.0009	0.0007
0.0008	-0.0021
-0.0009	0.0123
-0.0098	0.0132
-0.0005	-0.0056
-0.0011	0.0083
-0.0002	0.0009
-0.0025	0.0071
-0.0009	0.0068

=====

TOTAL (Rigid+flexible displacements) WORK-ENERGY TERMS

=====

WattHours	in-lbs
-----	-----

Elastic Energy:	6.009836e-001	1.914692e+004
Kinetic Energy:	3.871332e-005	1.233380e+000
Aerodynamic Damping work:	-2.477911e-001	-7.894454e+003
Aerodynamic Stifness work:	6.439095e-002	2.051451e+003
Actuator work:	4.082117e-001	1.300534e+004

TOTAL WORK-ENERGY BALANCE CHECK

LHS	RHS
1.330515e+004	1.300534e+004

This may not balance for the Control-Design-Model
 But must balance for the Evaluation Model
 (to within integration accuracy for work terms)

=====
 Work-Energy Terms through RIGID BODY displacement
 =====

	WattHours	in-lbs
Elastic Energy:	0.000000e+000	0.000000e+000
Kinetic Energy:	3.863577e-005	1.230909e+000
Aerodynamic Damping work:	-1.863621e-001	-5.937366e+003
Aerodynamic Stifness work:	1.863476e-001	5.936907e+003
Actuator work:	4.139624e-005	1.318856e+000

RIGID-BODY MOTION WORK-ENERGY BALANCE CHECK

LHS	RHS
7.717235e-001	1.318856e+000

This will not balance for the CDM unless the work due to the rigid-elastic KE coupling term, which is not computed in the LHS above, vanishes. The coupling term always vanishes in the EVM, therefore it must balance for the EVM!

=====
 Work-Energy Terms through FLEXIBLE displacements
 =====

	WattHours	in-lbs
Elastic Energy:	6.009836e-001	1.914692e+004
Kinetic Energy:	7.755646e-008	2.470895e-003
Aerodynamic Damping work:	-6.142907e-002	-1.957088e+003
Aerodynamic Stifness work:	-1.219567e-001	-3.885456e+003
Actuator work:	4.081703e-001	1.300402e+004

ELASTIC MOTION WORK-ENERGY BALANCE CHECK

LHS	RHS
1.330438e+004	1.300402e+004

This will not balance in the CDM unless the work due to the rigid-elastic KE coupling term, which is not computed in the LHS above, vanishes. The coupling term always vanishes in the EVM, therefore it must balance for the EVM!

TOTAL WORK-ENERGY BALANCE CHECK AGAIN

LHS
1.330515e+004

RHS
1.300534e+004

This may not balance for the Control-Design-Model
But must balance for the Evaluation Model
(to within integration accuracy for work terms)

Final Output Value (Maneuver Rate) for Control-Design-Model

GALAX-IMSC: 1.57

Final Values of Control Inputs:

GALAX-IMSC(modal) | GALAX-IMSC(generalized)

1.616484724e-013	0.000000000e+000
-7.476526637e+002	-4.078996466e+003
-2.700892496e+002	-1.874301228e+003
2.845134045e-001	2.353470681e+004
-8.487943460e-001	6.698051514e+002
-2.074230199e+000	5.015824569e+003
-3.593678776e+000	-1.568564148e+004
7.858741267e-004	4.265529426e+004
-1.185607202e-002	7.079831511e+004
2.989456908e-003	6.260184144e+004
6.513289563e-002	1.191514186e+005
1.572490235e+000	7.210945426e+003
-5.535256582e-001	1.792879923e+004
4.266172342e-002	-4.353475087e+004
8.050180883e+000	1.236593848e+004
-6.912366131e+000	5.923082176e+003
-3.949162041e+000	0.000000000e+000
3.672323859e-001	0.000000000e+000
1.487922429e+003	0.000000000e+000
-7.693182233e+002	0.000000000e+000
-3.222837215e+003	0.000000000e+000
-1.310386518e+003	0.000000000e+000
-3.919368654e+003	0.000000000e+000
1.778663325e+003	0.000000000e+000
6.198124680e+003	0.000000000e+000
2.702375601e+003	0.000000000e+000
4.633490701e+002	0.000000000e+000
3.079380000e+002	0.000000000e+000

-4.402487588e+002	0.000000000e+000
2.015381542e+003	0.000000000e+000
5.263106810e-001	0.000000000e+000
-6.116635423e+000	0.000000000e+000

GALAX-IMSC(real)

2.570960447e+005
-3.143222886e+006
2.509995410e+006
9.163781506e+006
-6.162849039e+006
-6.476191581e+006
2.562765623e+006
-7.309058765e+006
-5.190073685e+006
-1.044222389e+005
1.568842689e+006
1.641079810e+006
2.347820141e+006
2.311818562e+006

~~~~~  
ENERGY-WORK FOR GALAX-IMSC DESIGN (Control-Design-Model)  
~~~~~

Final Generalized Velocities Final Generalized Displacements
=====

1.5690	0.0003
-0.0203	-5.3373
0.0228	0.1311
0.0515	-0.3291
0.0033	-0.0052
0.0269	0.0134
-0.0229	0.0642
-0.0009	0.0007
0.0008	-0.0021
-0.0009	0.0123
-0.0098	0.0132
-0.0005	-0.0056
-0.0011	0.0083
-0.0002	0.0009
-0.0025	0.0071
-0.0009	0.0068

=====
TOTAL (Rigid+flexible displacements) WORK-ENERGY TERMS
=====

	WattHours	in-lbs
Elastic Energy:	6.009836e-001	1.914692e+004
Kinetic Energy:	3.871332e-005	1.233380e+000
Aerodynamic Damping work:	-2.477911e-001	-7.894454e+003
Aerodynamic Stifness work:	6.439095e-002	2.051451e+003

Actuator work: 2.650354e-001 8.443845e+003

TOTAL WORK-ENERGY BALANCE CHECK

LHS RHS
1.330515e+004 8.443845e+003

This may not balance for the Control-Design-Model
But must balance for the Evaluation Model
(to within integration accuracy for work terms)

=====
Work-Energy Terms through RIGID BODY displacement
=====

	WattHours	in-lbs
Elastic Energy:	0.000000e+000	0.000000e+000
Kinetic Energy:	3.863577e-005	1.230909e+000
Aerodynamic Damping work:	-1.863621e-001	-5.937366e+003
Aerodynamic Stifness work:	1.863476e-001	5.936907e+003
Actuator work:	0.000000e+000	0.000000e+000

RIGID-BODY MOTION WORK-ENERGY BALANCE CHECK

LHS RHS
7.717235e-001 0.000000e+000

This will not balance for the CDM unless the work due to the rigid-elastic KE coupling term, which is not computed in the LHS above, vanishes. The coupling term always vanishes in the EVM, therefore it must balance for the EVM!

=====
Work-Energy Terms through FLEXIBLE displacements
=====

	WattHours	in-lbs
Elastic Energy:	6.009836e-001	1.914692e+004
Kinetic Energy:	7.755646e-008	2.470895e-003
Aerodynamic Damping work:	-6.142907e-002	-1.957088e+003
Aerodynamic Stifness work:	-1.219567e-001	-3.885456e+003
Actuator work:	2.650354e-001	8.443845e+003

ELASTIC MOTION WORK-ENERGY BALANCE CHECK

LHS RHS
1.330438e+004 8.443845e+003

This will not balance in the CDM unless the work due to the rigid-elastic KE coupling term, which is not computed in the LHS above, vanishes. The coupling term always vanishes in the EVM, therefore it must balance for the EVM!

TOTAL WORK-ENERGY BALANCE CHECK AGAIN

LHS	RHS
1.330515e+004	8.443845e+003

This may not balance for the Control-Design-Model
But must balance for the Evaluation Model
(to within integration accuracy for work terms)

~~~~~  
DPCL-IMSC POWER  
~~~~~

Distributed-Parameter IMSC total power (via integration upto t-final):

1.586586e+003 KWatts 1.404058815442e+007 in-lbs/sec

Distributed-Parameter IMSC transient power(via Lyapunov):

1.566835e+002 KWatts 1.386579682028e+006 in-lbs/sec

~~~~~  
GALAX-IMSC POWER  
~~~~~

GALAX-IMSC modal power (via integration upto t-final):

1.589623e+003 KWatts 1.406745770633e+007 in-lbs/sec

GALAX-IMSC real power (via integration upto t-final):

1.885100e+006 KWatts 1.668230432452e+010 in-lbs/sec

GALAX-IMSC modal transient power (via Lyapunov):

1.566001e+002 KWatts 1.385841749253e+006 in-lbs/sec

GALAX-IMSC real transient power(via Lyapunov):

1.853676e+005 KWatts 1.640421508048e+009 in-lbs/sec

Do you want Evaluation Model Simulation?
 (enter 1(yes) or 0 (no)) :1

Final Output Value (Maneuver Rate) for Evaluation Model

Design-IMSC: 1.57 Synthesized DPCL-IMSC: 1.5715

For OPAX/GALAX-IMSC: 1.5725

=====

***** EVALUATION MODEL *****

=====

~~~~~

ENERGY-WORK FOR IMSC-SYNTHESIZED DISTRIBUTED-PARAMETER CONTROL  
 (EVM = Evaluation Model)

~~~~~

Final Generalized Velocities	Final Generalized Displacements
1.5701	2.0138
-0.0174	-5.3370
0.0009	0.1304
-0.0011	-0.3290
-0.0002	-0.0052
0.0001	0.0135
0.0003	0.0643
0.0001	0.0007
0.0000	-0.0021
0.0000	0.0123
0.0002	0.0132
0.0000	-0.0056
0.0000	0.0083
0.0000	0.0009
0.0001	0.0071
0.0000	0.0068

=====

TOTAL (Rigid+flexible displacements) WORK-ENERGY TERMS

=====

	WattHours	in-lbs
Elastic Energy:	6.008971e-001	1.914417e+004
Kinetic Energy:	3.869166e-005	1.232690e+000
Aerodynamic Damping work:	-2.500632e-001	-7.966842e+003

Aerodynamic Stifness work:	5.878614e-002	1.872886e+003
Actuator work:	4.096587e-001	1.305144e+004

TOTAL WORK-ENERGY BALANCE CHECK

LHS	RHS
1.305144e+004	1.305144e+004

This may not balance for the Control-Design-Model
 But must balance for the Evaluation Model
 (to within integration accuracy for work terms)

=====
 Work-Energy Terms through RIGID BODY displacement
 =====

	WattHours	in-lbs
Elastic Energy:	0.000000e+000	0.000000e+000
Kinetic Energy:	3.868685e-005	1.232536e+000
Aerodynamic Damping work:	-1.866849e-001	-5.947653e+003
Aerodynamic Stifness work:	1.866877e-001	5.947741e+003
Actuator work:	4.143211e-005	1.319998e+000

RIGID-BODY MOTION WORK-ENERGY BALANCE CHECK

LHS	RHS
1.320001e+000	1.319998e+000

This will not balance for the CDM unless the work due to the rigid-elastic KE coupling term, which is not computed in the LHS above, vanishes. The coupling term always vanishes in the EVM, therefore it must balance for the EVM!

=====
 Work-Energy Terms through FLEXIBLE displacements
 =====

	WattHours	in-lbs
Elastic Energy:	6.008971e-001	1.914417e+004
Kinetic Energy:	4.812188e-009	1.533130e-004
Aerodynamic Damping work:	-6.337828e-002	-2.019188e+003
Aerodynamic Stifness work:	-1.279015e-001	-4.074855e+003
Actuator work:	4.096173e-001	1.305012e+004

ELASTIC MOTION WORK-ENERGY BALANCE CHECK

LHS	RHS
1.305012e+004	1.305012e+004

This will not balance in the CDM unless the work due to the rigid-elastic KE coupling term, which is not computed in the LHS above, vanishes.
 The coupling term always vanishes in the EVM, therefore it must balance for the EVM!

TOTAL WORK-ENERGY BALANCE CHECK AGAIN

LHS	RHS
1.305144e+004	1.305144e+004

This may not balance for the Control-Design-Model
 But must balance for the Evaluation Model
 (to within integration accuracy for work terms)

~~~~~  
 ENERGY-WORK FOR GALAX DESIGN (Evaluation Model)  
 ~~~~~

Final Generalized Velocities Final Generalized Displacements

1.5677	2.0151
-0.1535	-5.3234
-0.1371	0.1087
-1.3050	-0.1045
-0.0817	-0.0056
-0.2234	0.0752
1.3374	-0.0805
1.5571	0.6702
2.6409	0.8340
-4.1896	0.7879
-5.2735	1.1794
-0.1809	0.0694
-0.2892	0.1327
-1.0959	-0.1981
-0.6936	0.1250
-0.3284	0.0669

=====

TOTAL (Rigid+flexible displacements) WORK-ENERGY TERMS

=====

	WattHours	in-lbs
Elastic Energy:	5.383159e+000	1.715037e+005
Kinetic Energy:	9.842534e-004	3.135763e+001
Aerodynamic Damping work:	-2.869731e-001	-9.142763e+003
Aerodynamic Stiffness work:	-2.481116e-001	-7.904663e+003
Actuator work:	4.849834e+000	1.545124e+005

TOTAL WORK-ENERGY BALANCE CHECK

LHS	RHS
1.544876e+005	1.545124e+005

This may not balance for the Control-Design-Model
 But must balance for the Evaluation Model
 (to within integration accuracy for work terms)

=====
 Work-Energy Terms through RIGID BODY displacement
 =====

	WattHours	in-lbs
Elastic Energy:	0.000000e+000	0.000000e+000
Kinetic Energy:	3.856915e-005	1.228786e+000
Aerodynamic Damping work:	-1.869376e-001	-5.955703e+003
Aerodynamic Stifness work:	1.868990e-001	5.954474e+003
Actuator work:	0.000000e+000	0.000000e+000

RIGID-BODY MOTION WORK-ENERGY BALANCE CHECK

LHS	RHS
-4.862057e-005	0.000000e+000

This will not balance for the CDM unless the work due to the rigid-elastic KE coupling term, which is not computed in the LHS above, vanishes. The coupling term always vanishes in the EVM, therefore it must balance for the EVM!

=====
 Work-Energy Terms through FLEXIBLE displacements
 =====

	WattHours	in-lbs
Elastic Energy:	5.383159e+000	1.715037e+005
Kinetic Energy:	9.456842e-004	3.012885e+001
Aerodynamic Damping work:	-1.000354e-001	-3.187060e+003
Aerodynamic Stifness work:	-4.350106e-001	-1.385914e+004
Actuator work:	4.849834e+000	1.545124e+005

ELASTIC MOTION WORK-ENERGY BALANCE CHECK

LHS	RHS
1.544876e+005	1.545124e+005

This will not balance in the CDM unless the work due to the rigid-elastic KE coupling term, which is not computed in the LHS above, vanishes. The coupling term always vanishes in the EVM, therefore it must balance for the EVM!

TOTAL WORK-ENERGY BALANCE CHECK AGAIN

LHS	RHS
1.544876e+005	1.545124e+005

This may not balance for the Control-Design-Model
 But must balance for the Evaluation Model
 (to within integration accuracy for work terms)

APPENDIX B : DPCL-IMSC COMPUTER RESULTS FOR HIGH-SPEED WING
 VIA OPTIMUM MODAL PERFORMANCE OUTPUT ALLOCATION FOR MODES 1,2,6

 MATLAB PROGRAM FOR AEROSERVOELASTIC MANEUVER VIA MODAL SYNTHESIS
 #####

 AEROELASTIC MODAL ANALYSIS AND DISTRIBUTED-PARAMETER MODAL CONTROL VIA IMSC

-- The units are {inches, pound-force and seconds} unless noted otherwise --

Air density (slug/ft³) : 0.001267
 Flight Speed : 24888 in/sec 2275.7587 km/hr
 DYNAMIC PRESSURE (psi): 18.9235

 Aeroelastic Eigenvalues (rad/sec or 1/sec)

Real Part	Imaginary Part
3.85581e-012	-9.16743e-016
2.03628e+003	8.77400e-014
-6.66482e-003	3.02105e+001
-6.66482e-003	-3.02105e+001
-8.69003e+000	8.63252e+001
-8.69003e+000	-8.63252e+001
7.65623e+000	8.65307e+001
7.65623e+000	-8.65307e+001
-1.04895e-003	1.23540e+002
-1.04895e-003	-1.23540e+002
5.11588e+000	1.50083e+002
5.11588e+000	-1.50083e+002
-5.24335e+000	1.50347e+002
-5.24335e+000	-1.50347e+002
-2.61625e-002	2.32295e+002
-2.61625e-002	-2.32295e+002
-1.76546e-002	2.80759e+002
-1.76546e-002	-2.80759e+002
-6.65399e-004	2.86147e+002
-6.65399e-004	-2.86147e+002
-5.03253e-002	3.18735e+002
-5.03253e-002	-3.18735e+002
5.12004e-003	3.43830e+002
5.12004e-003	-3.43830e+002
-3.16203e-002	4.26258e+002
-3.16203e-002	-4.26258e+002
-1.96150e-003	4.62506e+002

```

-1.96150e-003      -4.62506e+002
-3.28350e-001      4.76166e+002
-3.28350e-001      -4.76166e+002
3.31144e-001       4.94864e+002
3.31144e-001       -4.94864e+002

```

Modes Selected (modsel) for Control-Design-Model (wrt the order above)

```

1      2      4      6      12     16

```

Modal Control-Design Methods (selections below are wrt the modsel):

... LQR(Linear Quadratic Regulator) Design is used ...

The LQR weighting matrices for Modal Controllers

State Weightings | Compensator State Weightings | Control Weightings

```

1.00000e+000      1.00000e+002      1.00000e-004

```

!!!Modal Compensators ARE implemented!!!

Compensator matrices for Modal Controllers

```

ac      |      bc      |      gc      |      kc
-1.00000e-004  1.00000e+000  1.00000e+000  0.00000e+000

```

NON-PISAS means composite compensator and modal dynamics,
All gains are designed by either LQR or EVA

NON-PISAS Modes: 1 2 3 4 5 6

Method for Modal Synthesis of the Distributed-Parameter Control is: METHOD=1

Aeroservoelastic Closed-Loop Eigenvalues of the Control-Design-Model

***** DESIGN-IMSC ***** SYNTHESIZED-IMSC *****

(rad/sec or 1/sec):			
Real Part	Imaginary Part	Real Part	Imaginary Part
-2.04980e+003	0.00000e+000	-2.04980e+003	0.00000e+000
-1.14638e+000	0.00000e+000	-1.07584e+001	4.94965e+002
-8.71524e+000	3.16349e+001	-1.07584e+001	-4.94965e+002
-8.71524e+000	-3.16349e+001	-5.24078e+000	3.43867e+002
-4.92715e+000	0.00000e+000	-5.24078e+000	-3.43867e+002
-1.82064e+001	8.53780e+001	-7.36541e+000	1.49992e+002
-1.82064e+001	-8.53780e+001	-7.36541e+000	-1.49992e+002
-1.32155e+000	0.00000e+000	-1.82064e+001	8.53780e+001
-7.36541e+000	1.49992e+002	-1.82064e+001	-8.53780e+001
-7.36541e+000	-1.49992e+002	-8.71524e+000	3.16349e+001
-6.82840e-002	0.00000e+000	-8.71524e+000	-3.16349e+001
-5.24078e+000	3.43867e+002	-4.92714e+000	0.00000e+000
-5.24078e+000	-3.43867e+002	-1.14638e+000	0.00000e+000
-2.99871e-001	0.00000e+000	-1.32156e+000	0.00000e+000
-1.07584e+001	4.94965e+002	-6.82796e-002	0.00000e+000
-1.07584e+001	-4.94965e+002	-4.19364e-001	0.00000e+000
-4.19365e-001	0.00000e+000	-2.99874e-001	0.00000e+000

=====

IMSC Apparent Transient Modal Power and Gain Norms

=====

Design-IMSC:

Fro (Power)	Trace (Power)	Fro (Modal Gain)
1.45479e+008	1.67784e+008	1.12372e+004

Synthesized-IMSC:

Fro (Power)	Trace (Power)	Fro (Modal Gain)
1.45479e+008	1.67786e+008	1.12385e+004

IMSC True Transient Modal Power Norms

=====

Synthesized-IMSC		Design-IMSC	
-----		-----	
Fro(Power)	Trace(Power)	Fro(Power)	Trace(Power)
5.11708e+010	5.88578e+010	5.12000e+010	5.76813e+010
Alternate calculation			
5.11708e+010	5.88578e+010		

SIMULATIONS, CONTROL POWER AND ENERGY-WORK QUANTITIES:
#####

Output Performance Allocation: Do you want to optimize?

Enter 1 to optimize, enter 0 for user assignment : 1

COMMANDED OUTPUT ALLOCATION OPTIMIZATION

Real Control Power Weighting: 1e-010
Strain Energy Weighting: 1e-005

Desired Maneuver Rate (rad/sec): 1.57

Enter number of output Performance modes:3
(must be less than the number of controlled modes)

Select the performance modes [row vector] : [1 2 4]

Optimum Output Performance Objective Function: 0.00038326
Optimum Constraint value (Tolerance e-04): 2.8866e-015

Commanded Reference is: 1.57

Optimum Commanded Reference Allocation for Modal Controllers:

1.56049 0.00334 0.00618

Allocation sum (must be equal to Commanded Reference): 1.57

Optimum % Output Performance Allocation for Modal Controllers:

99.39406 0.21261 0.00000 0.39333 0.00000 0.00000

Allocation sum (must be equal to 100%): 100

Do you want Control Model Simulation?

enter 1(yes) or 0 (no) :1

Final Output Value (Maneuver Rate) for Control-Design-Model

Design-IMSC: 1.5699 Synthesized DPCL-IMSC: 1.5699

Final Values of Control Inputs:

Design-IMSC(modal) | Syn. DPCL-IMSC(modal) | Syn. DPCL-IMSC(generalized)

-1.352137365e+003	-1.352137365e+003	-3.181257117e+003
-1.589607471e+000	-1.468770044e+000	7.712363822e+002
-5.742459218e-001	-9.038938195e-001	-2.501587394e+002
0.000000000e+000	-3.813897619e+000	6.854499964e+002
0.000000000e+000	1.137807458e+001	5.875050130e+001
-4.104144265e+001	6.924172141e+000	1.957808885e+002
-9.030002436e+001	-7.197863418e+000	9.761577699e+002
0.000000000e+000	-9.465165393e-002	-3.520386071e+002
0.000000000e+000	1.427960008e+000	1.798106900e+002
0.000000000e+000	-7.299864747e-001	1.848150349e+002
0.000000000e+000	-1.590460554e+001	-1.212447447e+003
1.529378330e+000	1.573207685e+000	8.119482010e+001
0.000000000e+000	-1.628932089e+000	-1.742210184e+002
0.000000000e+000	9.695128691e-011	-9.842519072e+001
0.000000000e+000	-5.916993052e-001	-8.294003685e+002
0.000000000e+000	-9.136239227e-012	1.164815842e+003
0.000000000e+000	-5.829472478e+000	0.000000000e+000
0.000000000e+000	-6.939380750e-011	0.000000000e+000
0.000000000e+000	-3.790357260e+000	0.000000000e+000
0.000000000e+000	1.328740664e-010	0.000000000e+000
0.000000000e+000	3.156902248e+000	0.000000000e+000
0.000000000e+000	-5.920811899e-011	0.000000000e+000
0.000000000e+000	-3.749020207e+000	0.000000000e+000
0.000000000e+000	-4.397959640e-011	0.000000000e+000
0.000000000e+000	4.561786634e+001	0.000000000e+000
0.000000000e+000	-2.287478657e-010	0.000000000e+000
0.000000000e+000	2.290590637e+000	0.000000000e+000
0.000000000e+000	-1.319175845e-011	0.000000000e+000
0.000000000e+000	-9.314512499e-001	0.000000000e+000
0.000000000e+000	-6.410163698e-011	0.000000000e+000
0.000000000e+000	5.833539938e+000	0.000000000e+000

0.000000000e+000 3.775641962e-010 0.000000000e+000

~~~~~  
ENERGY-WORK FOR IMSC-SYNTHESIZED DISTRIBUTED-PARAMETER CONTROL  
(CDM = Control-Design-Model)  
~~~~~

Final Generalized Velocities Final Generalized Displacements
=====

1.5510	0.0003
-0.0734	-0.0064
-0.0055	-0.0115
0.3154	-0.0039
-0.0223	-0.0001
0.1695	-0.0030
-0.2241	0.0031
0.1771	-0.0001
-0.0450	-0.0001
-0.0533	0.0004
0.9268	0.0007
0.0345	0.0008
0.1174	0.0000
0.0452	0.0000
0.3528	0.0002
0.0844	0.0007

=====

TOTAL (Rigid+flexible displacements) WORK-ENERGY TERMS

=====

	WattHours	in-lbs
Elastic Energy:	3.046371e-005	9.705528e-001
Kinetic Energy:	5.702869e-005	1.816895e+000
Aerodynamic Damping work:	-6.205414e-001	-1.977002e+004
Aerodynamic Stifness work:	-3.089463e-003	-9.842817e+001
Actuator work:	-5.532794e-001	-1.762710e+004

TOTAL WORK-ENERGY BALANCE CHECK

LHS	RHS
-1.986566e+004	-1.762710e+004

This may not balance for the Control-Design-Model
But must balance for the Evaluation Model
(to within integration accuracy for work terms)

=====

Work-Energy Terms through RIGID BODY displacement

=====

	WattHours	in-lbs
Elastic Energy:	0.000000e+000	0.000000e+000
Kinetic Energy:	3.775460e-005	1.202835e+000
Aerodynamic Damping work:	-4.222619e-001	-1.345297e+004

Aerodynamic Stifness work: -2.257744e-004 -7.193017e+000
 Actuator work: -4.227049e-001 -1.346709e+004

RIGID-BODY MOTION WORK-ENERGY BALANCE CHECK

LHS	RHS
-1.345896e+004	-1.346709e+004

This will not balance for the CDM unless the work due to the rigid-elastic KE coupling term, which is not computed in the LHS above, vanishes.

The coupling term always vanishes in the EVM, therefore it must balance for the EVM!

=====
 Work-Energy Terms through FLEXIBLE displacements
 =====

	WattHours	in-lbs
Elastic Energy:	3.046371e-005	9.705528e-001
Kinetic Energy:	1.927410e-005	6.140594e-001
Aerodynamic Damping work:	-1.982796e-001	-6.317051e+003
Aerodynamic Stifness work:	-2.863689e-003	-9.123515e+001
Actuator work:	-1.305745e-001	-4.160013e+003

ELASTIC MOTION WORK-ENERGY BALANCE CHECK

LHS	RHS
-6.406702e+003	-4.160013e+003

This will not balance in the CDM unless the work due to the rigid-elastic KE coupling term, which is not computed in the LHS above, vanishes.

The coupling term always vanishes in the EVM, therefore it must balance for the EVM!

TOTAL WORK-ENERGY BALANCE CHECK AGAIN

LHS	RHS
-1.986566e+004	-1.762710e+004

This may not balance for the Control-Design-Model
 But must balance for the Evaluation Model
 (to within integration accuracy for work terms)

~~~~~  
 DPCL-IMSC POWER  
 ~~~~~

Distributed-Parameter IMSC total power (via integration upto t-final): 4 secs

3.113367e+003 KWatts 2.755192371664e+007 in-lbs/sec

Distributed-Parameter IMSC transient power(via Lyapunov):

4.214844e+002 KWatts 3.729950471472e+006 in-lbs/sec

Do you want Evaluation Model Simulation?
(enter 1(yes) or 0 (no)) :1

Final Output Value(Maneuver Rate)for Evaluation Model

Design-IMSC: 1.5699 Synthesized DPCL-IMSC: 1.5732

=====

***** EVALUATION MODEL *****

=====

~~~~~

ENERGY-WORK FOR IMSC-SYNTHESIZED DISTRIBUTED-PARAMETER CONTROL  
(EVM = Evaluation Model)

~~~~~

Final Generalized Velocities	Final Generalized Displacements
1.5531	4.8939
0.0005	-0.0059
-0.0008	-0.0128
-0.0013	-0.0024
0.0004	0.0003
0.0000	-0.0024
0.0009	0.0030
-0.0003	-0.0007
-0.0011	0.0010
-0.0003	0.0001
-0.0065	0.0078
-0.0004	0.0010
-0.0001	0.0006
0.0000	0.0000
-0.0006	0.0009
-0.0007	0.0010

=====

TOTAL (Rigid+flexible displacements) WORK-ENERGY TERMS

=====

	WattHours	in-lbs
Elastic Energy:	1.424030e-004	4.536860e+000
Kinetic Energy:	3.785864e-005	1.206150e+000
Aerodynamic Damping work:	-4.220500e-001	-1.344622e+004
Aerodynamic Stifness work:	-6.752648e-004	-2.151347e+001
Actuator work:	-4.225450e-001	-1.346199e+004

TOTAL WORK-ENERGY BALANCE CHECK

LHS	RHS
-1.346199e+004	-1.346199e+004

This may not balance for the Control-Design-Model
 But must balance for the Evaluation Model
 (to within integration accuracy for work terms)

=====

Work-Energy Terms through RIGID BODY displacement

=====

	WattHours	in-lbs
Elastic Energy:	0.000000e+000	0.000000e+000
Kinetic Energy:	3.785789e-005	1.206126e+000
Aerodynamic Damping work:	-4.218981e-001	-1.344138e+004
Aerodynamic Stifness work:	-6.599688e-004	-2.102615e+001
Actuator work:	-4.225202e-001	-1.346120e+004

RIGID-BODY MOTION WORK-ENERGY BALANCE CHECK

LHS	RHS
-1.346120e+004	-1.346120e+004

This will not balance for the CDM unless the work due to the
 rigid-elastic KE coupling term, which is not computed in the LHS above,
 vanishes.

The coupling term always vanishes in the EVM, therefore it must balance for the
 EVM!

=====

Work-Energy Terms through FLEXIBLE displacements

=====

	WattHours	in-lbs
Elastic Energy:	1.424030e-004	4.536860e+000
Kinetic Energy:	7.505271e-010	2.391128e-005
Aerodynamic Damping work:	-1.519494e-004	-4.841003e+000
Aerodynamic Stifness work:	-1.529601e-005	-4.873202e-001
Actuator work:	-2.484396e-005	-7.915113e-001

ELASTIC MOTION WORK-ENERGY BALANCE CHECK

LHS	RHS
-7.914387e-001	-7.915113e-001

This will not balance in the CDM unless the work due to the rigid-elastic KE coupling term, which is not computed in the LHS above, vanishes.

The coupling term always vanishes in the EVM, therefore it must balance for the EVM!

TOTAL WORK-ENERGY BALANCE CHECK AGAIN

LHS	RHS
-1.346199e+004	-1.346199e+004

This may not balance for the Control-Design-Model
But must balance for the Evaluation Model
(to within integration accuracy for work terms)